Probe Report

Title: Potent Anti-Diabetic Actions of a Novel Non-Agonist PPARγ Ligand that Blocks Cdk5-Mediated Phosphorylation.

Authors: Theodore M. Kamenecka[1], Scott A. Busby[2], Naresh Kumar[2], Jang Hyun Choi[3], Alexander S. Banks[3], Dušica Vidovic[4], Cameron M[2], Stephan C. Schurer[4], Becky A. Mercer[5], Peter Hodder[2,5], Bruce M. Spiegelman[3], and Patrick R. Griffin[2,6]

Affiliations: [1]Department of Chemistry, Scripps Florida, 130 Scripps Way, Jupiter, FL 33458; [2]Department of Molecular Therapeutics, Scripps Florida, 130 Scripps Way, Jupiter, FL 33458; [3]Department of Cancer Biology and Division of Metabolism and Chronic Disease, Dana-Farber Cancer Institute and Department of Cell Biology, Harvard Medical School, Boston MA 02115; [4]Center for Computational Science, University of Miami, 1120 NW 14th Street, Miami, FL 33136; [5]Lead Identification, Translational Research Institute, Scripps Florida, C130 Scripps Way, Jupiter, FL 33458; [6]Corresponding author: pgriffin@scripps.edu

Assigned Assay Grant #: MH079861-01

Screening Center Name & PI: Scripps Research Institute Molecular Screening Center (SRIMSC), H. Rosen

Chemistry Center Name & PI: SRIMSC, H. Rosen

Assay Submitter & Institution: Patrick R. Griffin, The Scripps Research Institute (TSRI)

PubChem Summary Bioassay Identifier (AID): 1808

Abstract

The incidence of diabetes is increasing rapidly as the percentage of the population ages and becomes more obese. According to the National Center for Health Statistics diabetes is now the sixth leading cause of death in the US. The biguanide metformin is typically the first-line medication used for treatment of type 2 diabetes mellitus (T2DM) as safety concerns over the use of the thiazolidinedione class [(TZD); rosiglitazone (Avandia) and pioglitazone (Actos) [1]] of insulin sensitizers has grown. This is unfortunate as TZDs have consistently shown robust efficacy for treatment of T2DM. TZDs target the nuclear receptor peroxisome proliferator-activated receptor gamma (PPARγ) and are classified as full agonists. While weight gain is associated with use of TZDs, the major safety concerns include edema, plasma volume expansion (PVE or hemodilution) which is likely linked to cardiomegaly and increased risk of congestive heart failure, and an increased risk of bone fractures. The latter risk is most troublesome as detection is typically only made when a patient suffers a fracture. Studies in animal models and in clinical trials have shown that indicators of weight gain and PVE, while not eliminated, can be minimized without loss of insulin sensitization by the use of modulators that are weak or partial agonists of PPARγ (e.g., minimal agonism of the receptor as compared to TZDs). Partial agonists have been referred to as selective PPARγ modulators or SPPARγMs and this class of ligand has been shown to have a different binding mode in the PPARγ ligand binding pocket (LBP) as compared to the full agonists [2]. Selective recruitment of transcriptional coactivators by partial agonists has also been demonstrated. A combination of different ligand binding mode and distinct coactivator recruitment profile may explain the change in gene expression patterns compared to that of full agonists [3]. While it is unclear if the bone fracture risk has been minimized with use of such agents, these studies clearly demonstrate that the anti-diabetic efficacy of partial agonists is uncoupled from their transcriptional activity but does correlate well with binding potency. Recently we have shown that many PPARγ-based drugs have a separate

biochemical activity, blocking the obesity-linked phosphorylation of PPARγ by Cdk5. Due to their improved adverse event profile of partial agonists and the observation of separate biochemical activities of PPARγ ligands, we sought to develop compounds with high affinity binding to PPARγ but that lacked classical agonism and block the Cdk5-mediated phosphorylation in cultured adipocytes and in insulin-resistant mice. Here we describe one such compound, ML244, which has a unique mode of binding to PPARγ, has potent anti-diabetic activity while not causing the fluid retention and weight gain that are serious side effects of many of the PPARγ drugs. Unlike TZDs, ML244 does not interfere with bone formation in culture. These data illustrate that new classes of anti-diabetes drugs can be developed by specifically targeting the Cdk5-mediated phosphorylation of PPARγ.

Probe Structure & Characteristics

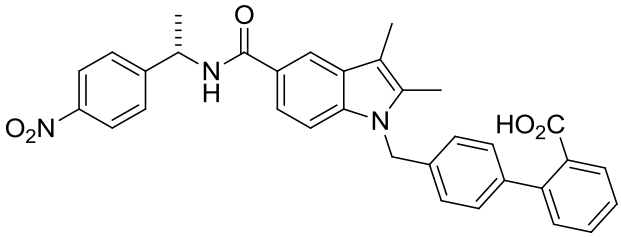

PPARγ Non-Agonist Probe
ML244
SR-03000001664
CID 53239856/ SID 124349301

CID/ML	Target	EC50 [SID, AID]	Anti-Target	EC50 [SID, AID]	Fold Selective	Secondary Assays: EC50 (nM) [SID, AID]
NEW Probe: CID 53239856 / ML244	PPARγ Lantha Binding Assay	80 nM [SID 124349301, AID 504943] Active	PPARα	>10 µM [SID 124349301] Inactive	>125	**PPRE::Luc Transactivation Reporter Assay**: Inactive [SID 124349301, AID 504939] Probe is a ligand, non agonist. **Inhibition of Cdk5-Mediated PPARγ Phosphorylation**: Active [SID124349301, AID 504938] **Efficacy Studies: Reductions in Ob/Ob Mouse Glucose and Insulin Levels**: Active [SID124349301, AID 540293]. **Modulation of Adipocyte Differentiation Genes**: Inactive [SID124349301, AID 540286 (Ap2); 540289 (PPARγ); 540290 (CD36); 540291 (LPL); 540292 (FASN); 540294 (Glut4)] **Modulation of Osteoblast Differentiation Genes**: Inactive [SID 124349301, 540282 (PPARγ); AID 540283 (RANKL); 540284 (COLI); 540285 (Alp)]
Old Probe: CID 1328217/ ML215		194 nM [SID 91762765, (AID 504446] Active	PPARα	>3 µM [SID 91762765, AID 504735] Inactive	>10.6	**PPRE::Luc Transactivation Assay (2X%INH):** 48% of Rosi and 98% of MRL-24 activity; [SID 91762765, AID 504452] Active. Old probe is a partial agonist. **PPRE::Luc Dose Response Assay:** 0.283 µM [SID 91762765, AID 504447] Active **PPARγ PolarScreen Binding Assay:** 152 nM [SID 91762765, AID 504453] Active.

Recommendations for Scientific Use of the Probe

Limitations in state of the art. The clinical use of PPARγ agonists has been associated with adverse effects that are mainly caused by the concomitant activation of various target genes implicated in different physiological pathways. Current state of the art include thiazolidinediones (TZDs; also known as glitazones, which include rosiglitazone and pioglitazone), a class of medicines used to treat type 2 diabetes introduced in the 1990s, which act by binding to the receptor. Additional ligands for PPARγ include eicosanoids and free fatty acids. Several side effects have been associated with the use of TZDs, including water retention, edema,

which may lead to heart failure in certain individuals. Further, one of the newer TZDs, pioglitazone has been suggested to contribute to bladder cancer in some patients. Interestingly partial or weak agonists have been shown to have similar efficacy as full agonist TZDs yet they exhibit an improved side effect profile. There are many examples of partial agonists that have entered clinical development including AMG131 (INT131), MBX102, MK0533, as well as many others. However, most if not all of these published partial agonists still maintain significant transactivation (TA) activity of PPARγ. Recently we have shown that many anti-diabetic PPARγ ligands of the TZD and other chemical classes have a second, distinct biochemical function: blocking the obesity-linked phosphorylation of PPARγ by cyclin-dependent kinase 5 (Cdk5) at serine 273. This is a direct action of the ligands and requires binding to the PPARγ ligand binding domain (LBD), causing a conformational change that interferes with the ability of Cdk5 to phosphorylate serine 273. Rosiglitazone and MRL24 (a selective partial agonist toward PPARγ) both modulate serine 273 phosphorylation at therapeutic doses in mice. Furthermore, a small clinical trial of newly diagnosed type 2 diabetics showed a remarkably close association in individual patients between the clinical effects of rosiglitazone and the blocking of this phosphorylation of PPARγ [4]. Thus, the contribution made by classical agonism to the therapeutic effects of these drugs and to their side effects is not clear. These data suggest that it might be possible to develop entirely new classes of anti-diabetes drugs optimized for the inhibition of Cdk5-mediated phosphorylation of PPARγ while lacking classical agonism. Here we describe the development of synthetic small molecules that bind tightly to PPARγ yet are completely devoid of classical agonism and effectively inhibit phosphorylation at serine 273. These compounds have a unique binding mode in the ligand binding pocket of PPARγ. An example from this series, ML244, exhibits potent and dose-dependent anti-diabetic effects in obese mice. Unlike TZDs and other PPARγ agonists, this compound does not cause fluid retention or weight gain *in vivo* or reduce osteoblast mineralization in culture. To date there are no publications of potent binding non-agonists of PPARγ that block S273 phosphorylation and that have been shown to have potent anti-diabetic activity. Thus the pharmacology of ML244 is very unique.

Probe Applications. The probe can be used to dissect the role of classical agonism of PPARγ versus blocking the cdk5 phosphorylation of the receptor in adipogenesis, insulin sensitization, and lipid metabolism. The probe can also be used in proteomic studies to determine the difference members of the transcriptional complex when activated by full agonist, partial agonist, or non-agonists.

*Expected end-users of the probe in the research community***.** The probe can be used by academic researchers studying insulin sensitivity and diabetes pathology. It is conceivable that scientists in diverse fields will be able to apply this chemical probe to elucidate the role of PPARγ in various cellular pathways. Our lab already has several collaborators using this probe. For example, Michael Mancini's lab at Baylor College of Medicine is using the probe and analogs to look at PPARγ trafficking within cell adipocytes in response to full and partial agonist activation. Bruce Spiegelman at Dana Farber and Harvard School of Medicine has done extensive studies with this novel PPARγ probe.

Relevant biology of the probe. PPARγ is a nuclear receptor that functions as a ligand-dependent transcriptional regulator of multiple genes involved in adipogenesis, insulin sensitization and lipid metabolism. PPARγ is required for adipogenesis. PPARs are obligate heterodimers with the retinoid X receptors (RXRs) and these heterodimers regulate transcription of an array of PPAR target genes. Partial agonists as compared to full agonists are reported to show fewer side effects in preclinical models of diabetes, while retaining similar pharmacodynamic efficacy as TZDs. However, any level of classical activation of PPARγ is likely to drive PVE and modulation of bone formation. Thus there is substantial interest in identification of PPARγ modulators with as minimal as possible classical activation of PPARγ while maintaining robust antidiabetic efficacy. ML244

represents an excellent chemical starting point as a potent binder to PPARγ that is completely devoid of classical agonism of the receptor.

1 Introduction

Development of novel PPARγ ligands

In order to develop a suitable ligand, we optimized compounds for (*i*) high binding affinity for PPARγ *(ii)* blocking the Cdk5-mediated PPARγ phosphorylation and *(iii)* lacking classical agonism. We first identified published compounds that bind tightly to PPARγ and have favorable properties as a scaffold for extensive chemical modifications. Classical agonism is defined here, as is standard in the nuclear receptor field, as an increased level of transcription through a tandem PPAR response element luciferase reporter (PPRE::Luc). Of particular interest was compound **7b** described by Lamotte et al. as an extremely potent (EC_{50} hPPARγ ~800pM PPRE::LUC; IC_{50} hPPARγ 8nM competitive Lanthascreen) and selective PPARγ partial agonist (30% activation of the human receptor as compared to rosiglitazone)[5]. A modular synthesis approach was used to make a series of analogs of compound **7b**; these compounds were tested *in vitro* and in adipose cells. Using a LanthaScreen competitive binding assay, ML244 had an IC_{50} of 80nM (see Section 3.2). When compared to rosiglitazone or MRL24 (a partial agonist) in a classical transcriptional activity assay on a tandem PPRE::Luc reporter, ML244 had essentially no transcriptional agonism at any concentration (see section 3.2). Rosiglitazone and ML244 both effectively blocked the Cdk5-mediated phosphorylation of PPARγ *in vitro* with half-maximal effects between 20 and 200 nM (**Figure 1**). In contrast, they had no effect on the phosphorylation of a well-characterized Cdk5 substrate, the Rb protein [6]. This suggested that these compounds do not disrupt the basic protein kinase function of Cdk5. In addition, ML244 was also effective at blocking Cdk5-mediated phosphorylation of PPARγ in differentiated fat cells with no measurable difference in phosphorylation of Rb (see **Figure 1**). Additional analogs were synthesized and four compounds were identified that have similar *in vitro* profiles. These data demonstrate that several analogs can be made that potently block Cdk5-dependent phosphorylation of PPARγ in cells while demonstrating little to no classical agonism.

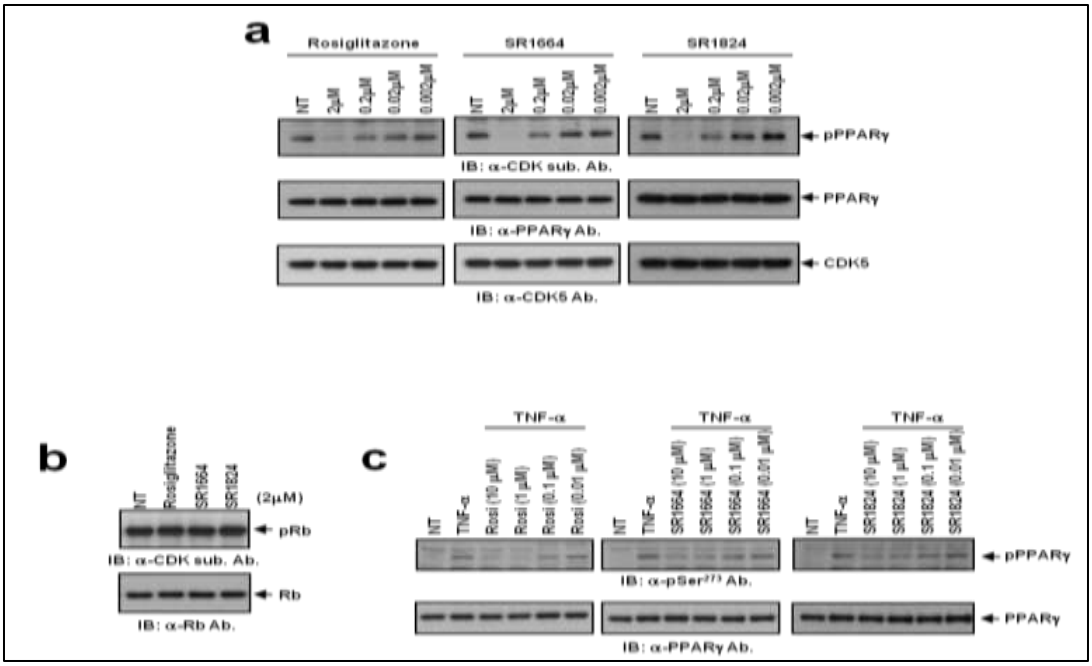

Figure 1. **a** and **b**, *in vitro* Cdk5 assay with rosiglitazone, ML244 or SR1824 with PPARγ or Rb substrates. **e**, TNF-α-induced phosphorylation of PPARγ in differentiated PPARγ KO MEFs expressing $PPAR\gamma^{WT}$ treated with rosiglitazone, ML244 or SR1824. These data are available as PubChem AID 504938.

Of the several compounds identified as non-agonist inhibitors of Cdk5-mediated PPARγ phosphorylation, ML244 had adequate pharmacokinetic properties to move forward to biological and therapeutic assays. Adipogenesis was the first known biological function of PPARγ [7] and agonist ligands for PPARγ have been shown to potently stimulate the differentiation of pre-adipose cell lines; this response has been widely used as a sensitive cellular test for PPARγ agonism [8-10]. Rosiglitazone (a full agonist) potently stimulated fat cell differentiation, as evidenced by Oil Red O staining of the cellular lipid (see Section 3.5). In contrast, ML244 did not stimulate increased lipid accumulation or changes in morphology characteristic of differentiating fat cells. The stimulation of fat cell gene expression was also apparent with rosiglitazone, as illustrated by an increased expression of *aP2*, *C/EBPα* and *Glut4* (see PubChem AIDs 540286, 540287, and 540294). In contrast, ML244 induced little or no change in the expression of these genes linked to adipogenesis (see Section 3.5).

Another well-known effect of both rosiglitazone and pioglitazone is that they decrease bone formation and bone mineral density leading to an increase in fracture risk [11, 12]. TZDs have also been shown to decrease bone mineralization in cultured osteoblasts [13]. Rosiglitazone treatment reduced the mineralization (calcification) of mouse osteoblastic cells (MC3T3-E1 cells), as measured by Alizarin red S staining (see Section 3.5). Moreover, the expression of genes involved in the differentiation of these cells was impaired (alkaline phosphatase (*Alp*), receptor activator of nuclear factor kappa-B ligand (*Rankl*) and type I collagen (*Col1*)) (see Section 3.5). Importantly, the treatment with ML244 did not affect the extent of calcification or the expression of this osteoblast gene set in MC3T3-E1 cells.

We next asked whether ML244 had anti-diabetic properties *in vivo*. Wild-type mice fed a calorie-dense diet high in sugar and fat become obese and insulin-resistant, with activation of Cdk5 in their adipose tissues [4]. Administration of ML244, injected twice daily for 5 days, caused a dose-dependent decrease in the Cdk5-mediated phosphorylation of PPARγ at serine 273 in adipose tissue (**Figure 2**). Moreover, ML244 treatment also caused a trend toward lowered (and normalized) glucose levels, and a significant reduction in the fasting insulin levels. Insulin resistance, as computed by HOMA-IR, showed a clear and dose-dependent improvement with ML244. These changes occurred without significant differences in body weight compared to vehicle treated mice (data not shown).

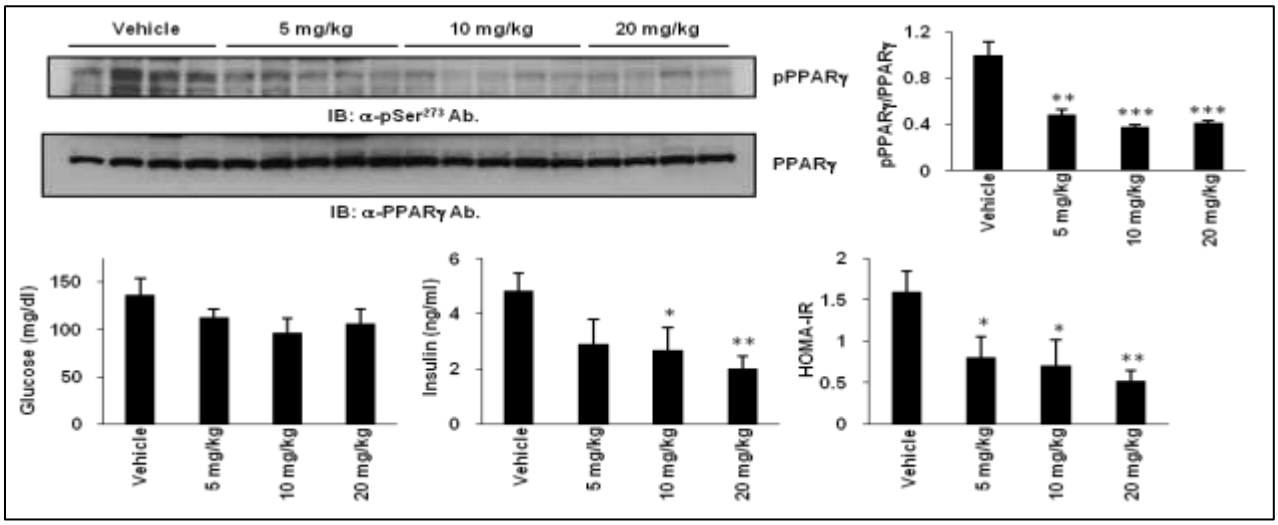

Figure 2. Anti-diabetic activity of ML244 in high-fat diet (HFD) mice. Dose-dependent inhibition of phosphorylation of PPARγ by ML244 in white adipose tissue (WAT). Quantification of PPARγ phosphorylation compared to total PPARγ (top right). *Ad libitum* fed glucose (p=0.062 at 10mg/kg), insulin and HOMA-IR in HFD mice (bottom).

A more severe model of obesity is the leptin-deficient ob/ob mouse. These animals are very obese and insulin-resistant, with substantial compensatory hyperinsulinemia. We performed preliminary pharmacokinetic and pharmacodynamic experiments comparing rosiglitazone and ML244 to determine dosing regimens. Comparable drug exposures were achieved with treatments of 40mg/kg for ML244 and 8mg/kg for rosiglitazone, both injected twice daily. Functional analyses were performed at days 5 and 11 after the start of treatments. Both drugs caused a similar reduction in PPARγ phosphorylation at S273 (data not shown). After five days of treatment, there were no overt differences in fasting body weight or glucose levels (see **Figure 3**). Mice receiving only the vehicle control remained hyperinsulinemic, but both rosiglitazone and ML244 substantially reduced these insulin levels (see **Figure 3**, left). Glucose tolerance tests were markedly improved with both rosiglitazone and ML244, and the areas under these glucose excursion curves were statistically indistinguishable, without changing body weight (see **Figure 3**, right). These glucose results are available as PubChem AID 540923.

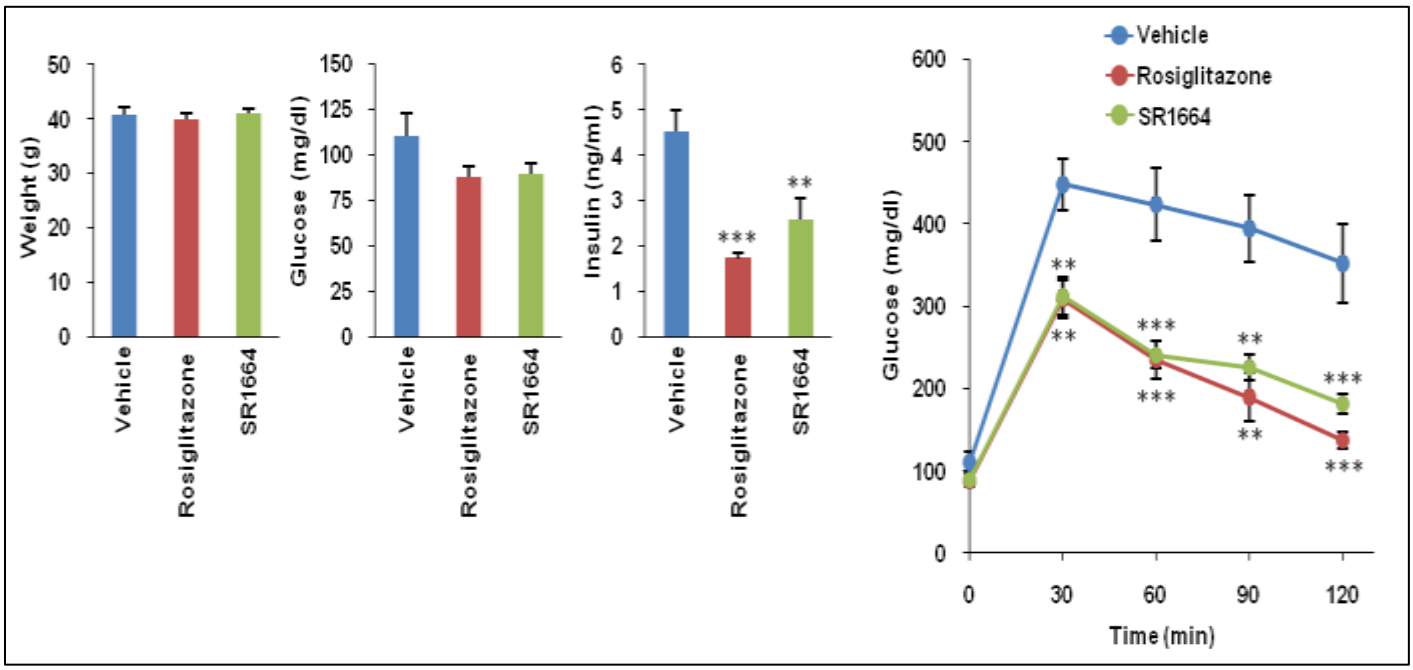

Figure 3. Fasting body weight, blood glucose and insulin levels prior to glucose-tolerance tests (GTT) in ob/ob mice treated with vehicle, rosiglitazone or ML244 (n=8).

While there is no definitive proof, weight gain and fluid retention caused by TZD drugs like rosiglitazone are suspected to be key factors in their increased cardiac risk [14, 15]. After recovering from the glucose tolerance test on day 5, rosiglitazone treated mice began to show an increase in body weight, an effect persisting for the duration of the experiment (see **Figure 4**, left panel). This increased mass is accounted for primarily by fluid retention, quantified by a characteristic decrease in hematocrit seen with hemodilution (see **Figure 4**, right panel). However, an increase in body fat can also contribute to weight gain and this was observed by MRI. Importantly, ML244 treatment did not cause the weight gain seen with the rosiglitazone treatment. Furthermore, ML244 treatment showed no decrease in the hematocrit or change in body adiposity. These results were confirmed by measurements showing a decreased concentration of hemoglobin in the mice treated with rosiglitazone but not those treated with ML244 (data not shown). Taken together, these data indicate that ML244, a non-agonist PPARγ ligand, has anti-diabetic actions in two murine models of insulin-resistance. Furthermore, this non-agonist does not stimulate two of the best documented side-effects of the PPARγ agonist drugs *in vivo.* These data suggest that ML244 is a significant advance over the current state-of-the-art in modulation of PPARγ for treatment of diabetes.

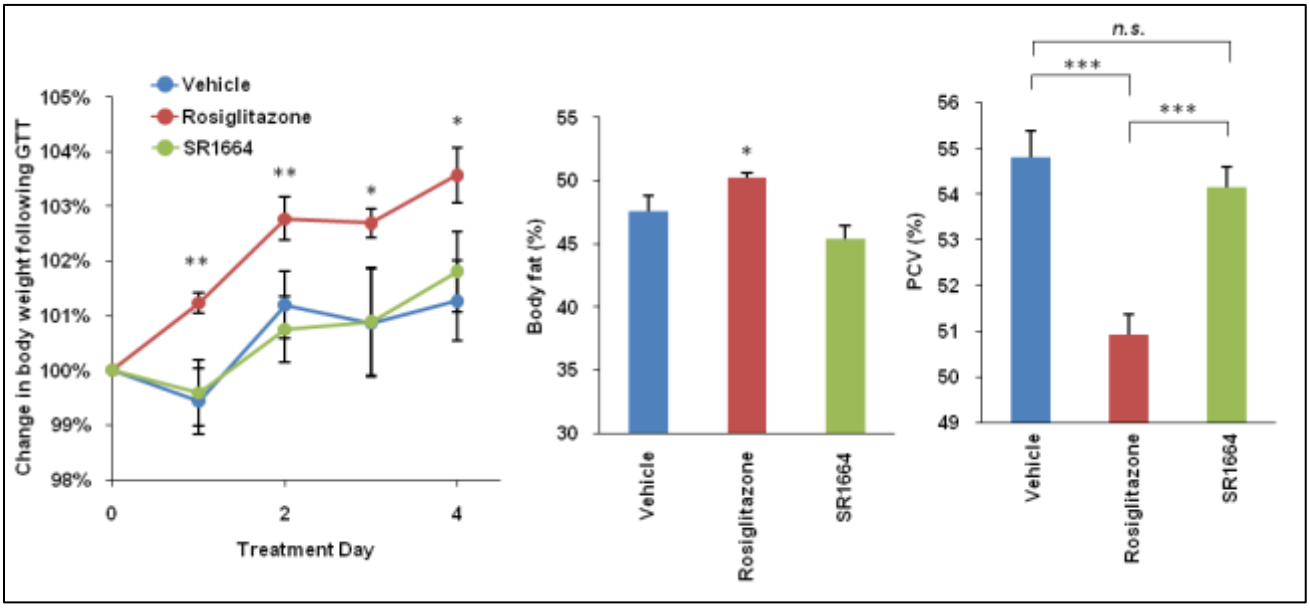

Figure 4. Whole-body weight (**left**) and fat change (**middle**) with continued drug administration following the GTT. (**right**) Packed cell volume (PCV) in whole blood from ob/ob mice treated with vehicle, rosiglitazone or ML244. Error bars are S.E.M; *p<0.05, **p<0.01, ***p<0.001. n.s.; not significant.

2.1 Assays

The assays performed by the SRIMSC and assay provider for this probe development project are reported in **Table 1**. Descriptions of the late stage assays are presented after the table.

Table 1. PubChem BioAssays

AID	Assay Name	Target	Powder Sample	Dose Tested	Compounds Tested/Active
631	HTS Primary Screen (HTRF)	PPARγ-SRC1	No	8 µM	196,256/ 811
1051	HTS Artifact Counterscreen	Artifacts	No	8 µM	99,367/ 335
1300	HTS Confirmation (HTRF)	PPARγ-SRC1	No	8 µM	794/ 454
1319	HTS Dose Response (HTRF)	PPARγ-SRC1	No	Range: 80µM-4nM	349/10
1679	HTS Dose Response Non-Sel AG (HTRF)	PPARγ-SRC1	No	Range: 80µM-4nM	400/ 75
1808	Summary of Project	PPARγ	N/A	N/A	N/A
504452	Primary PPARγ Assay (LUMI)	PPARγ	Yes	5 µM	235/ 60
504447	PPARγ Dose Response Assay (LUMI)	PPARγ	Yes	Range: 5µM-200pM	70/ 24
504453	PPARγ Polarscreen Assay	PPARγ	Yes	Range: 10µM-1nM	19/ 7
504446	PPARγ Lanthascreen Assay	PPARγ	Yes	Range: 5µM - 2nM	16/ 11
504938	Phospho-PPARγ Western Blot (CDK5)	P- PPARγ	Yes	2 µM	3/3
504939	PPRA Transactivation Assay	PPARγ	Yes	Range: 10µM to 0.033 nM	8/6
504943	PPARγ Lanthascreen Assay (Round 2)	PPARγ	Yes	Range: 1 µM to 0.033 nM	10/9
540282	PPARγ (Bone) QPCR	PPARγ	Yes	10 µM	1/0
540283	RANKL (Bone) QPCR	RANKL	Yes	10 µM	1/0
540284	Type I Collagen (COL1) (Bone) QPCR	COL1	Yes	10 µM	1/0
540285	Alkaline Phosphatase (ALP) (Bone) QPCR	ALP	Yes	10 µM	1/0
540286	Fatty Acid Binding Protein 4 (aP2) (Adipocyte) QPCR	Ap2	Yes	10 µM	1/0
540287	C/EBP-alpha (Adipocyte) QPCR	C/EBP-alpha	Yes	10 µM	1/0
540289	PPARγ (Adipocyte) QPCR	PPARγ	Yes	10 µM	1/0
540290	CD36 (Adipocyte) QPCR	CD36	Yes	10 µM	1/0
540291	Lipoprotein Lipase (Adipocyte) QPCR	LPL	Yes	10 µM	1/0
540292	Fatty Acid Synthase (Adipocyte) QPCR	FASN	Yes	10 µM	1/0
540293	Ob/Ob Leptin^{def} Mouse Glucose	PPARγ	Yes	10 µM	1/1
540294	GLUT4 (Adipocyte) QPCR	GLUT4	Yes	10 µM	1/0

PPARγ Activation Assays (PubChem AIDs 504452 , 504447, and 504939)

The purpose of this assay is to identify compounds that can increase the activity of PPARγ. In this assay, Cos-1 cells co-transfected with a full length PPARγamma (PPARγ) construct in a pSport6 vector backbone (pS6-hPPARγ) and three copies of a PPARγ response element (3x-PPRE)-luciferase reporter construct, are incubated for 20 hours with test compound. As designed, a compound that activates PPARγ activity will bind and activate the pS6-PPARγ construct, thereby stimulating PPARγ-mediated activation of the 3xPPRE-luciferase reporter, leading to an increase in well luminescence. Compounds were tested in duplicate at a final nominal concentration of 5 µM (*AID* 504452) and in triplicate using an 8-point titration series starting at a nominal concentration of 5 µM (range 5 µM to 0.002 µM) (AID 504447).

PPARγ Polarscreen (AID 504453)

The purpose of this biochemical assay is to identify compounds that can directly bind to PPARγ through competition with a fluorescently labeled high affinity PPARγ compound. The fluorescent ligand when bound to the PPARγ LBD protein has a constrained movement leading to a high fluorescence polarization value. When test compound displaces the fluorescent control compound, it causes this compound to tumble freely resulting in a low polarization value. This assay allows for the separation of compounds positive in the cell-based luminescence assays that are working through direct binding to PPARγ versus compounds modulating PPARγ transactivation activity through indirect mechanisms. Compounds are tested in triplicate using an 8-point titration series starting at a nominal concentration of 10 micromolar (range 10 micromolar to 1 nanomolar).

PPARγ Lanthascreen (AID 504446)

The purpose of this assay is to confirm compounds that can directly bind to PPARγ through competition with a fluorescently labeled high affinity PPARγ compound. The fluorescent ligand when bound to the PPARγ LBD protein is in close proximity to the Tb-anti PPARγ antibody bound to the N-terminal His tag on the PPARγ LBD. In the absence of test compound, this provides a robust TR-FRET signal which is the ratio of the fluorescein emission at 520nm and the Tb emission at 490nm. When test compound displaces the fluorescently labeled control compound, it causes a loss of the TR-FRET signal which is proportional to how much of the compound is displaced. This assay allows for the separation of compounds positive in the cell-based luminescence assays that are working through direct binding to PPARγ versus compounds modulating PPARγ transactivation activity through indirect mechanisms. In addition, it provides a more sensitive measurement of compound binding to PPARγ than the Polarscreen PPARγ Competitor assay based on head to head comparisons with positive controls such as Rosiglitazone. Therefore, positive hits from the above Polarscreen PPARγ competitor assay were also evaluated in this assay along with analogs to our probe SR-01000788129.

2.2 Probe Chemical Characterization

Probe chemical structure including stereochemistry. *Separation of diastereomers (if necessary)*.

The structure of the PPARγ non agonist probe ML244:

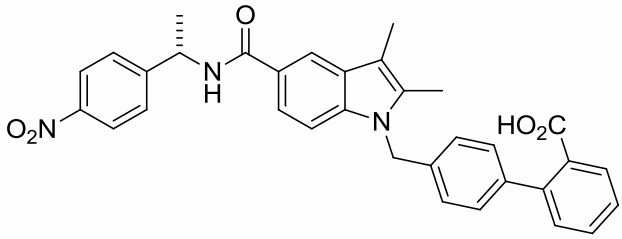

Structure verification with 1H NMR, 13CNMR, and LCMS results.

Probe ML244 was obtained as a near colorless foam with >98% purity (**HPLC analysis**): **^{1}H NMR** (400 MHz, DMSO-d_6): δ (ppm) 8.83 (d, J = 7.6Hz, 1H), 8.25 (m, 1H), 8.16 (d, J = 1.2 Hz, 1H), 7.74-7.68 (m, 4H), 7.57 (dt, J = 1.6, 7.2 Hz, 1H), 7.51 (d, J = 8.4 Hz, 1H), 7.46 (dt, J = 1.2, 7.2 Hz, 1H), 7.36 (dd, J = 0.8, 7.6 Hz, 1H), 7.28 (m, 2H), 7.03 (m, 2H), 5.52 (s, 2H), 5.32 (quint, J = 7.2 Hz, 1H), 2.36 (s, 3H), 2.34 (s, 3H), 1.57 (d, J = 6.8 Hz, 3H); **^{13}C NMR** (400 MHz, DMSO-d_6): δ (ppm) 170.5, 167.9, 154.5, 147.2, 141.5, 140.7, 138.7, 138.2, 135.1, 133.2, 131.8, 131.5, 130.0, 129.6, 128.6, 128.2, 128.1, 126.8, 125.8, 124.4, 121.4, 118.8, 109.7, 108.3, 49.4, 46.7, 22.9, 11.0, 9.7; HRMS (ESI) m/z 548.2187 [M+H]+ (calc M+H $C_{33}H_{29}N_3O_5$ 547.2107).

Solubility. The solubility of the probe was measured in phosphate buffered saline (PBS: 137 mM NaCl, 2.7 mM KCl, 10 mM sodium phosphate dibasic, 2 mM potassium phosphate monobasic and a pH of 7.4) at room

temperature (23°C). The solubility of probe ML244 was found to be >200 µM. The solubility increases at higher pH's due to the carboxylic acid moiety in the molecule.

Stability. The stability of the probe was measured at room temperature (23ºC) in PBS (no antioxidants or other protectants; DMSO concentration below 0.1%). The stability, represented by the half-life, was found to be >24 hours. These values were determined over a 24 hour period with a minimum of 6 time points.

The probe was measured for its ability to form glutathione adducts. At concentrations of 100 µM reduced GSH, 10 µM of the probe does not appear to be a Michael acceptor [16, 17].

Sample Preparation:	All compounds sampled after 20 hrs equilibration by rotation.
Standard Concentrations (HPLC):	100µM in 50/50 Acetonitrile/H_2O. Injected 25µL to HPLC
Standard Concentrations (LC/MS):	0.5µM in 50/50 Acetonitrile/H2O.
Compounds:	Sampled after centrifugation. Injected 50µL directly to HPLC.

Probe	SR Number	CID	SID	Solubility in PBS (µM)[1]	Stability in PBS $t_{1/2}$
ML244	SR-03000001664	53239856	124349301	*>200 µM*	>24 hours

[1]Solubility increases at higher pH (>7.4).

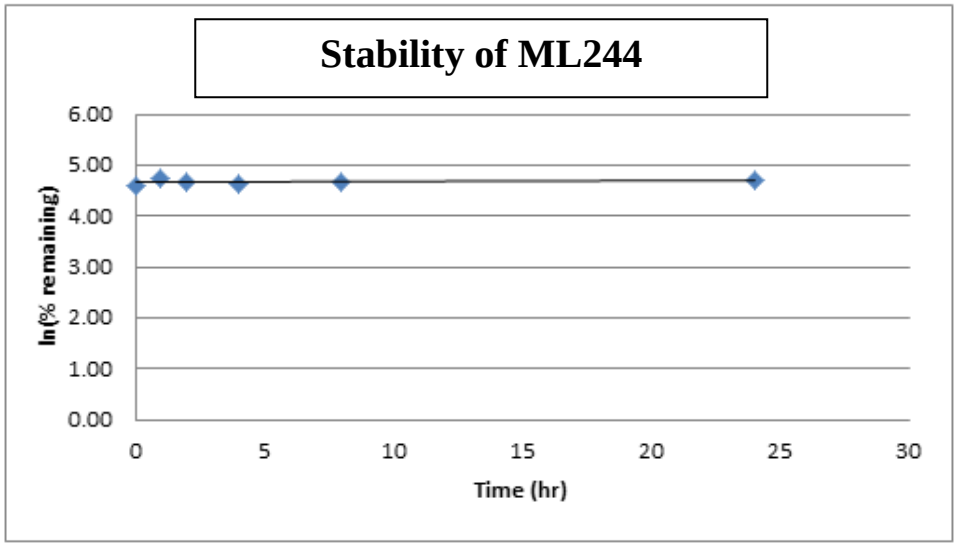

Figure 5. Stability of ML244.

2.3 Probe Preparation

Detailed experimental procedures for the synthesis of ***Probe ML244***

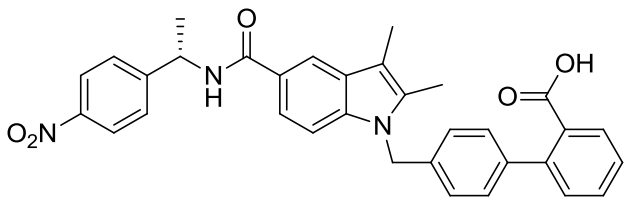

Step 1: *tert*-Butyl 2-bromobenzoate

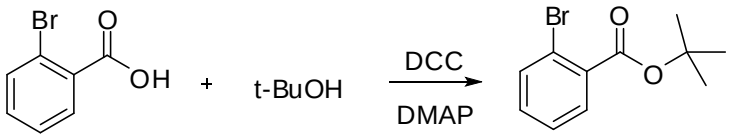

To a solution of 2-bromobenzoic acid (8.08 g, 40.2 mmol), DMAP (0.492 g, 8.0 mmol) and *t*-BuOH (9.3 mL, 80.4 mmol) in dry DCM (300 mL) under argon, was added DCC (9.96 g, 48.2 mmol). The reaction mixture was stirred at room temperature for 20 h. The resulting mixture was filtered and the filtrate was evaporated *in vacuo*. The crude mixture was dissolved in AcOEt (300 mL) and washed with saturated aqueous $NaHCO_3$ (x2), brine and then dried over Na_2SO_4. After filtration, solvent was evaporated. The crude product was purified by flash chromatography on silica gel (AcOEt/hexane 0->30%) to obtain the title compound.

Step 2: *tert*-Butyl 4'-methylbiphenyl-2-carboxylate

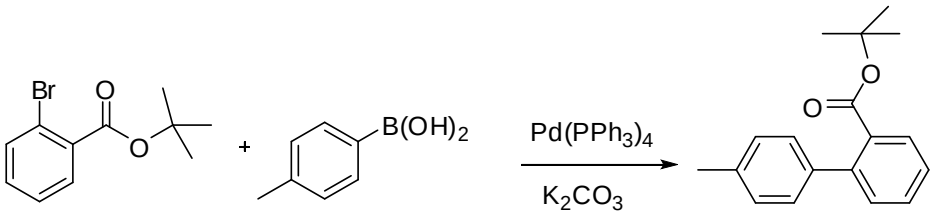

To a 350 mL high-pressure vial was added *tert*-butyl 2-bromobenzoate (5.142 g, 20.0 mmol), *p*-tolylboronic acid (4.08 g, 30.0 mmol), $Pd(PPh_3)_4$ (3.47 g, 3.0 mmol), potassium carbonate (8.29 g, 60.0 mmol) and dioxane with water (4:1, 200 mL). The mixture was degassed for 5 min and sealed. The mixture was heated at 100°C for 40 min wherein analytical HPLC analysis indicated the completion of the reaction. The mixture was filtered through Celite and MeOH was used to wash the Celite pad. The solvent was removed and the crude was purified by flash chromatography (AcOEt /Hexane 0->30%) to obtain the title compound.

Step 3: *tert*-butyl 4'-(bromomethyl)biphenyl-2-carboxylate

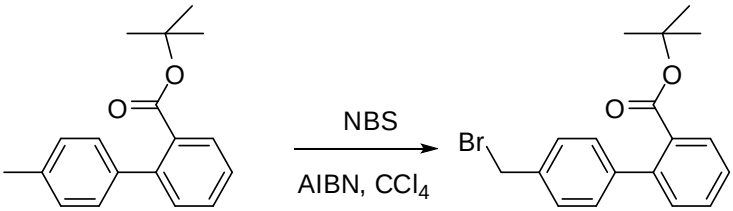

To a 500 mL round-bottom flask was added *tert*-butyl 4'-methylbiphenyl-2-carboxylate (7.04 g, 26.23 mmol), NBS (5.14 g, 28.85 mmol), AIBN (0.43 g, 2.62 mmol) and CCl_4 (200 mL). The reaction mixture was refluxed for 2h at 100°C. The completion of the reaction was monitored by analytical HPLC. The reaction mixture was allowed to cool to room temperature and filtered. The filtrate was concentrated to obtain the crude product which was purified by flash chromatography (AcOEt/Hexane 0->30%) to obtain the title compound.

Step 4: *tert*-Butyl 1-(4-(ethoxycarbonyl)phenyl)hydrazinecarboxylate

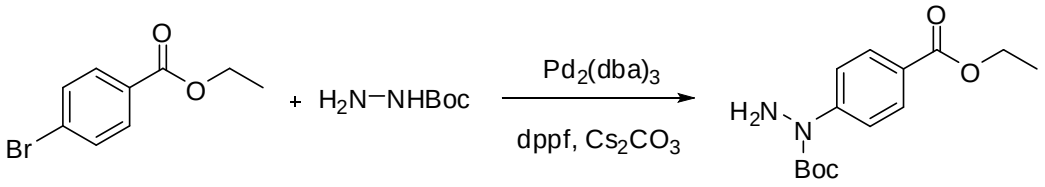

To a 350 mL high-pressure vial was added ethyl 4-bromobenzoate (12.92 g, 56.4 mmol), *t*-butyl carbazate (14.91 g, 112.8 mmol), $Pd_2(dba)_3$ (0.516 g, 0.56 mmol), dppf (0.938 g, 1.69 mmol), Cs_2CO_3 (18.4 g, 56.4 mmol), and dry toluene (113 mL). The reaction mixture was degassed for 5 min, sealed and heated to 100°C for 16 h. The completion of the reaction was monitored by analytical HPLC. The reaction mixture was allowed to cool to room temperature, diluted with DCM, filtered and the filtrate was concentrated. The crude was then purified by flash chromatography (AcOEt/Hexane (0->30%) to afford the desired product. ESI-MS (m/z): 265 $[M+H-NH_3]^+$, 225 $[M+H-tBu]^+$, 181 $[M+H-Boc]^+$. ^1H NMR (400 MHz, DMSO-d_6): δ (ppm) 1.31 (t, J = 7.1 Hz, 3H, CH_3 ethyl), 1.50 (s, 9H, CH_3 Boc), 4.28 (q, J = 7.1 Hz, 2H, CH_2 ethyl), 5.14 (s, 2H, NH_2), 7.70 (dt, J = 8.8, 2.2 Hz, 2H, H_2 and H_6 phenyl), 7.87 (dt, J = 8.8, 2.2 Hz, 2H, H_3 and H_5 phenyl).

Step 5: Ethyl 2,3-dimethyl-1*H*-indole-5-carboxylate

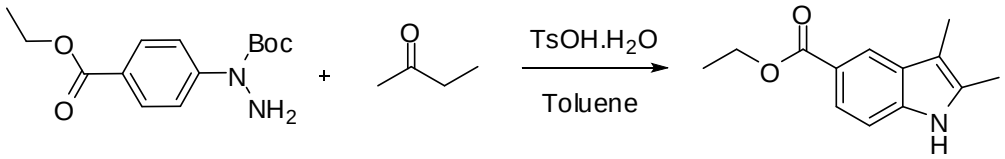

A mixture of *tert*-butyl 1-(4-(ethoxycarbonyl)phenyl)hydrazinecarboxylate (5.27 g, 18.8 mmol), butan-2-one (2.53 mL, 28.2 mmol), and TsOH monohydrate (21.5 g, 112.8 mmol) in toluene (300 mL) was heated at 80°C for 2h. The reaction mixture was allowed to cool to room temperature and filtered. The filtrate was concentrated and then purified by flash chromatography (AcOEt/Hexane 5%) to obtain the title compound. ESI-MS (m/z): 218 $[M+H]^+$; ^1H NMR (400 MHz, DMSO-d_6): δ (ppm) 1.33 (t, J = 7.2 Hz, 3H, CH_3 ethyl), 2.18 (s, 3H, CH_3), 2.32 (s, 3H, CH_3), 4.29 (q, J = 7.2 Hz, 2H, CH_2 ethyl), 7.28 (dd, J = 8.4, 0.4 Hz, 1H, H_7 indole), 7.64 (dd, J = 8.4, 1.6 Hz, 1H, H_6 indole), 8.05 (m, 1H, H_4 indole).

Step 6: Ethyl 1-((2'-(*tert*-butoxycarbonyl)biphenyl-4-yl)methyl)-2,3-dimethyl-1*H*-indole-5-carboxylate

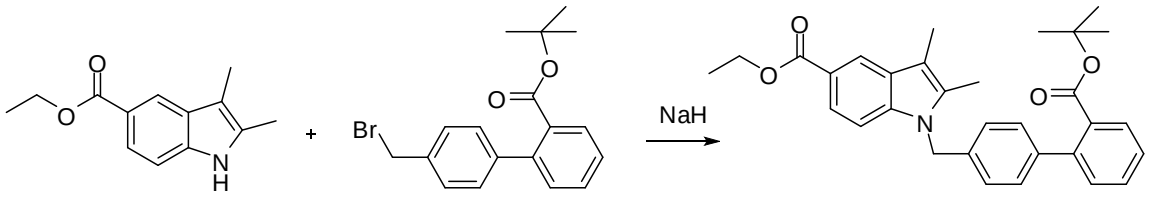

To a mixture of ethyl 2,3-dimethyl-1*H*-indole-5-carboxylate (1.493 g, 6.87 mmol) in dry DMF (10 mL) at 0°C under argon was added NaH (0.3 g, 60% dispersion in mineral oil, 7.56 mmol) in portions. The reaction mixture was stirred at rt for 30 min and then re-cooled to 0°C. *Tert*-butyl 4'-(bromomethyl)biphenyl-2-carboxylate (2.62 g, 7.56 mmol) in DMF (2 mL) was slowly added. The reaction mixture was stirred at rt for another 1h. The completion of the reaction was monitored by anal. HPLC. The reaction was quenched with MeOH, and then the solvent was removed *in vacuo*. The crude was dissolved in AcOEt, washed with saturated aqueous $NaHCO_3$, brine and dried over Na_2SO_4 and filtered. The filtrate was evaporated in *vacuo* to obtain the crude which was purified by flash chromatography (AcOEt/Hex 10->100%) to obtain the title compound. ESI-MS (m/z): 484 $[M+H]^+$.

Step 7: 1-((2'-(*tert*-Butoxycarbonyl)biphenyl-4-yl)methyl)-2,3-dimethyl-1*H*-indole-5-carboxylic acid

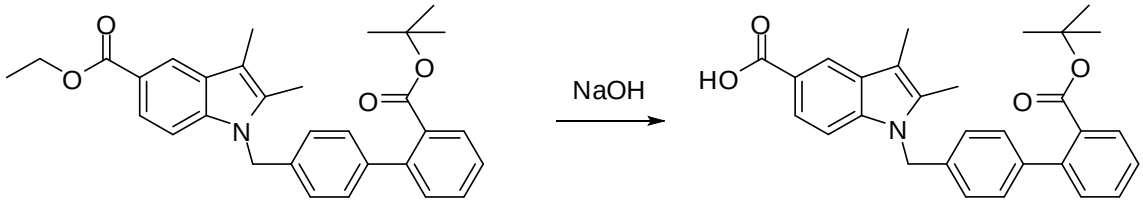

A mixture of ethyl 1-((2'-(*tert*-butoxycarbonyl)biphenyl-4-yl)methyl)-2,3-dimethyl-1*H*-indole-5-carboxylate (3.72 g, 7.69 mmol) and NaOH (7.7 mL, 2N, 15.4 mmol) in EtOH (30 mL) was refluxed at 100°C for 2h. The completion of the reaction was monitored by anal. HPLC. The reaction mixture was cooled to rt, then acidified to pH~4 with 2N HCl solution. The mixture was evaporated in *vacuo* to obtain the crude, which was precipitated from water and filtered to obtain the title compound. ESI-MS (m/z): 456 $[M+H]^+$; ^1H NMR (400 MHz, DMSO-d_6): δ (ppm) 1.13 (s, 9H, CH_3 tBu), 2.26 (s, 3H, CH_3 indole), 2.33 (s, 3H, CH_3 indole), 5.49 (s, 2H, CH_2-biphenyl), 7.01 (d, J = 8 Hz, 2H, H_7 and H_9 biphenyl), 7.19 (d, J = 8 Hz, 2H, H_6 and H_{10} biphenyl), 7.30 (d, J = 7.6 Hz, 1H, H_7 indole), 7.40-7.47 (m, 2H, H_2 and H_4 biphenyl), 7.53 (dt, J = 1.2, 7.6 Hz, 1H, H_3 biphenyl), 7.63-7.69 (m, 2H H_6 indole and H_5 biphenyl), 8.13 (d, J = 1.2 Hz, 1H, H_4 indole).

Step 8: (*S*)-*tert*-Butyl 4'-((5-(1-(4-nitrophenyl)ethylcarbamoyl)-2,3-dimethyl-1*H*-indol-1-yl)methyl)biphenyl-2-carboxylate

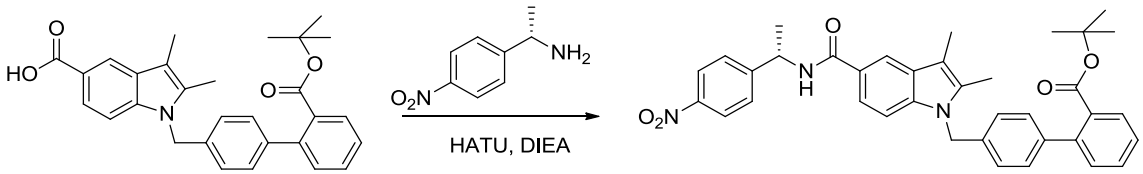

To a mixture of 1-((2'-(*tert*-butoxycarbonyl)biphenyl-4-yl)methyl)-2,3-dimethyl-1*H*-indole-5-carboxylic acid (46 mg, 0.1 mmol) in DMF (1 mL) was added DIEA (26 mg, 0.2 mmol) and HATU (46 mg, 0.12 mmol). The mixture was stirred for 5 min, and then (*S*)-1-(4-nitrophenyl)ethanamine (20 mg, 0.13 mmol) was added. The reaction mixture was stirred at rt for 30 min. The completion of the reaction was monitored by anal. HPLC. The solvent was removed *in vacuo* to obtain the crude which was purified by flash chromatography (AcOEt/Hex 10->100%) to obtain the title compound. ESI-MS (m/z): 576 $[M+H]^+$.

Step 9: (*S*)-4'-((5-(1-(4-nitrophenyl)ethylcarbamoyl)-2,3-dimethyl-1*H*-indol-1-yl)methyl)biphenyl-2-carboxylic acid

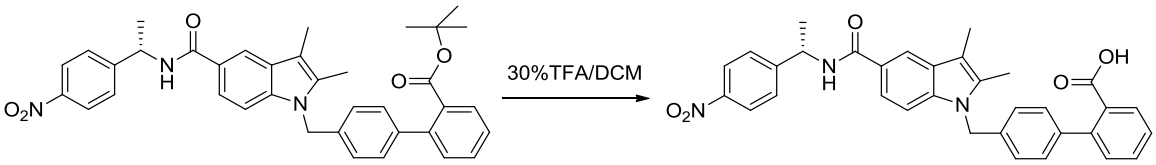

A mixture of (*S*)-*tert*-butyl 4'-((5-(1-(4-bromophenyl)ethylcarbamoyl)-2,3-dimethyl-1*H*-indol-1-yl)methyl)biphenyl-2-carboxylate (20 mg, 0.03 mmol) in TFA/DCM (1 mL, 30%) was stirred at rt for 2h. The completion of the reaction was monitored by anal. HPLC. The solvent was removed to obtain the crude which was purified by reverse phase prep-HPLC (MeOH/Acetonitrile/water) to obtain the title compound. ESI-MS (m/z): 548 $[M+H]^+$; HRMS (ESI) m/z 548.2187 [M+H]+ (calc M+H $C_{33}H_{29}N_3O_5$ 547.2107); ^1H NMR (400 MHz, DMSO-d_6): δ (ppm) 8.83 (d, J = 7.6Hz, 1H), 8.25 (m, 1H), 8.16 (d, J = 1.2 Hz, 1H), 7.74-7.68 (m, 4H), 7.57 (dt, J = 1.6, 7.2 Hz, 1H), 7.51 (d, J = 8.4 Hz, 1H), 7.46 (dt, J = 1.2, 7.2 Hz, 1H), 7.36 (dd, J = 0.8, 7.6 Hz, 1H), 7.28 (m, 2H), 7.03 (m, 2H), 5.52 (s, 2H), 5.32 (quint, J = 7.2 Hz, 1H), 2.36 (s, 3H), 2.34 (s, 3H), 1.57 (d, J = 6.8 Hz, 3H); ^{13}C NMR (400 MHz, DMSO-d_6): δ (ppm) 170.5, 167.9, 154.5, 147.2, 141.5, 140.7, 138.7, 138.2, 135.1, 133.2, 131.8, 131.5, 130.0, 129.6, 128.6, 128.2, 128.1, 126.8, 125.8, 124.4, 121.4, 118.8, 109.7, 108.3, 49.4, 46.7, 22.9, 11.0, 9.7.

3 Results

3.1 Summary of Screening Results

This Center-based effort arose out of a previous HTS campaign to identify selective agonists of the interaction PPARγ with the coactivators SRC1, SRC2, and SRC3 (see **Figure 6**). Unfortunately, these campaigns only identified compounds with EC50 values > 10 µM, which were not considered tractable. As a result, the SRMISC implemented a Center-based approach to explore the identification of partial or non-agonists of PPARγ.

Previous SRIMSC HTS Campaign for PPARγ/SRC selective agonists. No tractable leads identified.

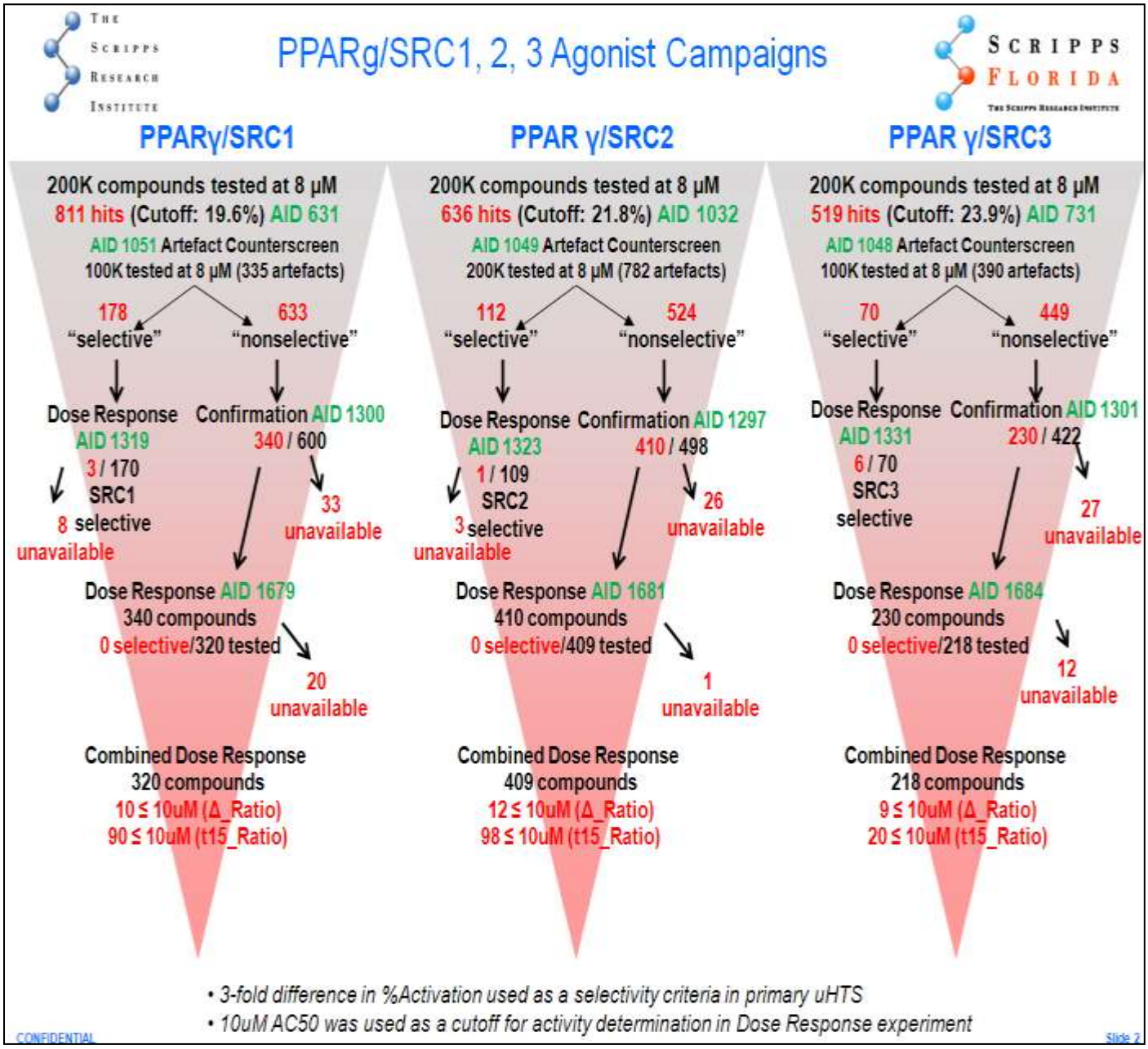

Figure 6. Cartoon showing the critical path of the High Throughput Screening (HTS) campaign hit selection process and numeric assay cutoffs.

3.2 Dose Response Curves for Probe

*Probe ML244 (*SR-03000001664; CID 53239856; SID 124349301; Synthesized).

We next assessed the ability of the probe to directly bind to PPARγ, a necessary feature of a ligand (**Figure 7**). We employed a biochemical assay (PolarScreen) that monitors the ability of the probe to compete with a fluorescently labeled high affinity PPARγ compound. The fluorescent ligand when bound to the PPARγ LBD protein has a constrained movement leading to a high fluorescence polarization value. When test compound displaces the fluorescent control compound, it causes this compound to tumble freely resulting in a low polarization value. This assay allows for the separation of compounds positive in the cell-based luminescence assays that are working through direct binding to PPARγ versus compounds modulating PPARγ transactivation activity through indirect mechanisms. Compounds were tested in triplicate using an 8-point titration series starting at a nominal concentration of 10 micromolar (range 10 micromolar to 1 nanomolar). The results of this assay show that probe ML244 does indeed bind to PPARγ (also see PubChem AID 504453).

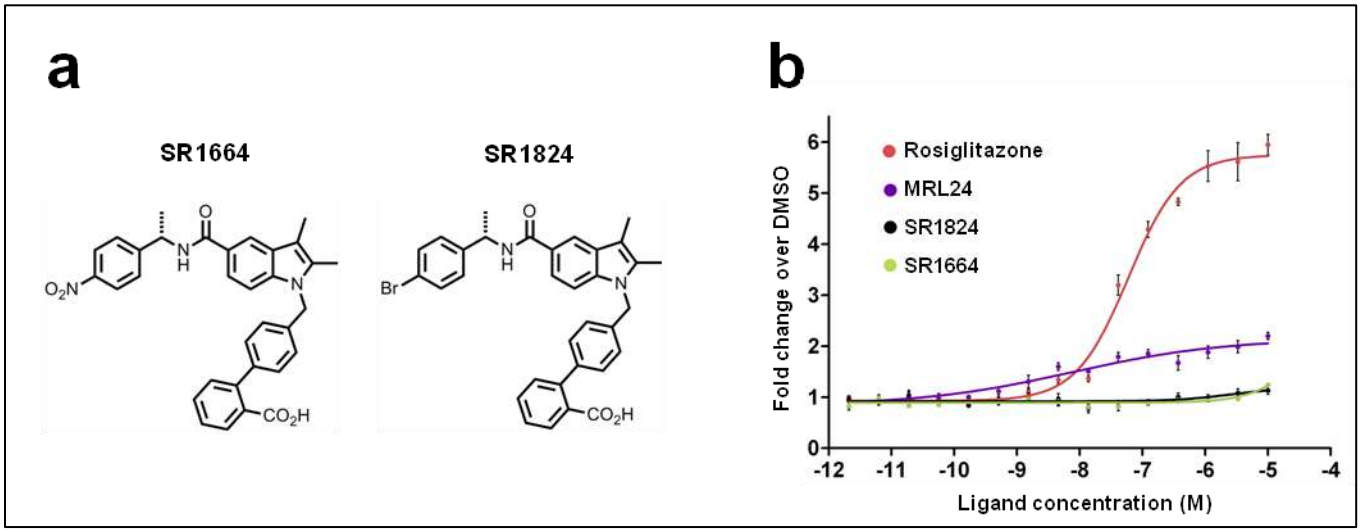

Figure 7. **a**, Chemical structures of ML244 and SR1824. **b**, Transcriptional activity of a PPAR-derived reporter gene in COS-1 cells following treatment with rosiglitazone, ML244 or SR1824 (n=3). These results are also available as PubChem AID 504453 (PolarScreen: binding assay).

We next employed **LanthaScreen** technology to distinguish compounds positive in the cell-based luminescence assays and PolarScreen that are working through direct binding to PPARγ versus compounds that modulate PPARγ transactivation activity through indirect mechanisms. In addition, LanthaScreen provides a more sensitive measurement of compound binding to PPARγ than the Polarscreen PPARγ Competitor assay, based on head to head comparisons with positive controls such as Rosiglitazone. Therefore, positive hits from the Polarscreen PPARγ competitor assay were also evaluated in this assay along with analogs to our probe ML244 (SID 91762765). As can be seen in **Figure 8**, the probe compounds performs in an almost identical manner as does rosiglitazone, demonstrating that the probe directly binds to PPARγ. Importantly, as shown in **Table 2**, the probe ML244 (SR-1664) does not activate the PPARγ response element (PPRE; also see PubChem AID 504939), indicating that it is non-agonist ligand. These features make the probe a desirable candidate as an insulin-sensitizing PPARγ modulator with minimal classical activation of PPARγ and reduced side effects, while maintaining robust antidiabetic efficacy.

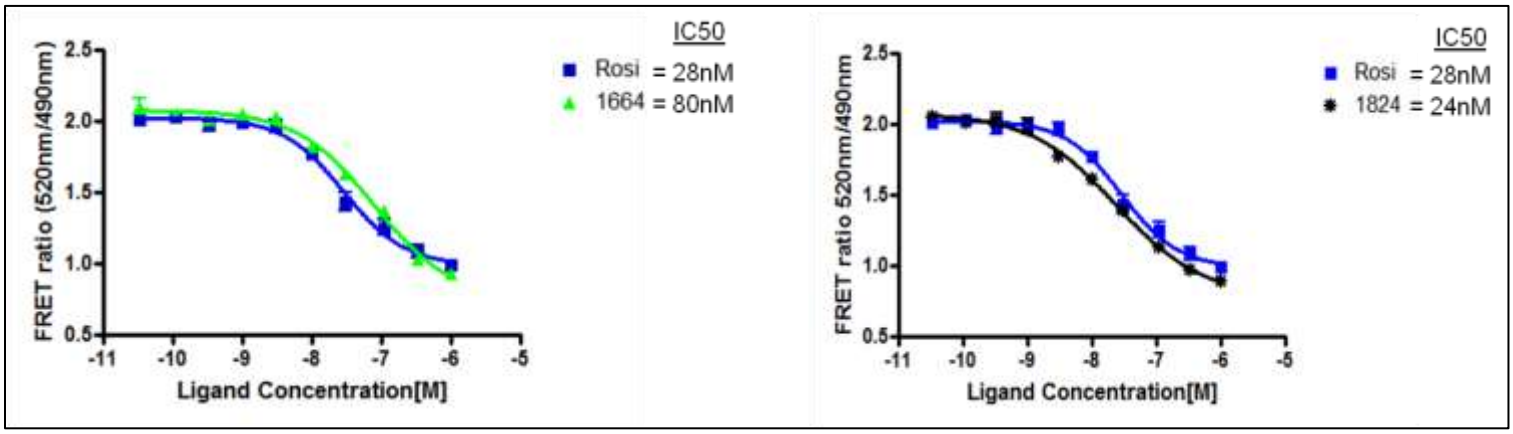

Figure 8. Dose response curves of ML244 (Left panel) and SR1824 (Right panel) as compared to rosiglitazone in the competitive Lanthascreen assay (n=3). These results are also available as PubChem AID 504446.

Compound	IC50 (binding affinity)	Ki	EC50 (PPRE) (%relative to rosiglitazone)
Rosiglitazone	18nM	6.45nM	7.4nM (100%)
Compound 7b	370pM	132.61pM	540nM (15%)
SR1663	2nM	716pM	20nM (23%)
SR1664	80nM	28.67nM	Not active (0%)
SR1665	466nM	167.02nM	3µM (7%)
SR1666	76nM	27.24nM	300nM (26%)
SR1701	13nM	4.65nM	2.7µM (20%)
SR1706	>1000nM		Not tested
SR1707	No binding		Not tested
SR1708	10nM	3.58nM	Not active (0%)
SR1713	No binding		Not tested
SR1714	17nM	6.09nM	> 1µM (9%)
SR1717	4nM	1.43nM	Not active (0%)
SR1824	28nM	10.03nM	Not active (0%)

Table 2. Binding affinity as determined in a competitive Lanthascreen assay (PubChem AID 504943) and transcriptional activity (PubChem AID 504939) of chemical derivatives of the Lamotte et al prior art compound **7b** from the literature.

3.3 Scaffold/Moiety Chemical Liabilities

Describe SAR & chemistry strategy (including structure and data) that led to the probe.

Probe ML244 was identified through SAR (structure activity relationship) of the potent PPARγ partial agonist SR-9034 recently published in the primary literature [5]. Modification of different parts of the molecule (**Figure 9**; **Table 3** on the next page) led to different in vitro properties.

Figure 9. SAR of Lead PPARγ partial agonist SR-9034

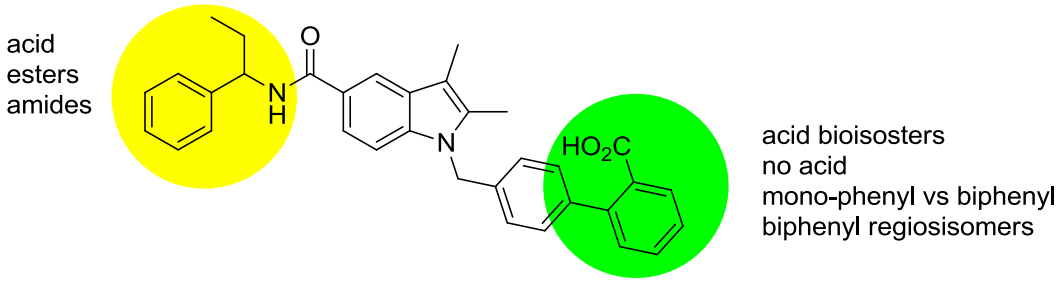

For instance, conversion of the alpha-phenethyl amide side chain in SR-9034 to the 4-nitrophenylethyl amide bearing the (S)-configuration at the chiral center led to a compound with no agonism of the receptor as measured in the cell based transactivation assay (SR-1664). This was also found for the 4-bromo analog SR-1824. Other substituted amides investigated, however, showed partial agonism. The amide is definitely required for potency, as truncation of the amide to an acid or ester leads to a large drop in potency (data not shown). The nature of the interactions of the differently substituted indole amides is currently under investigation using a combination of methods including X-ray crystal structures, HD-exchange and molecular modeling. Further SAR is required to fully understand the effect of substitution on the level of agonism of the receptor.

Modifications to the biphenyl carboxylic acid moiety were also investigated. The carboxylic acid was not absolutely required for potency as the corresponding tetrazole (SR-2049) as well as nitrile (SR-2046) were equally active in vitro. These modifications did not seem to effect on the level of agonism of PPARγ. Another interesting and unexpected finding was that the biphenyl acid did not need to be in the 1,4-relationship, as in 9034. From X-ray crystal structures of potent partial agonists of PPARγ (MRL24 and 9034), the carboxylic acid residue forms a key hydrogen bond with Ser342 in the receptor. With the biphenyl rings in a 1,3-relationship, the carboxylic acid at the meta (SR-2220) and para (SR-2222) position both give potent partial agonists. It is not clear if the acid moiety can still form the same key interaction with Ser342. Nonetheless, most of these analogs are potent partial agonists of PPARγ. Also surprising, was the fact that the second phenyl ring and acid were not even required for potency (SR-1991). Shortened analogs of this type were all potent partial agonists. In these cases, it's not clear of the binding mode to the receptor. They could be flipped in the receptor, as was found for the analog of MRL24, MRL20 [18].

Nine (9) analogs of ML244 have been synthesized to date, with two of them being potent binders of PPARγ and showing no agonism of the receptor in the cell based transactivation assay. All other analogs synthesized have been potent binders, as well as partial agonists of PPARγ.

3.4 SAR Tables

Table 3. In vitro profile of SR-9034 Analogs.

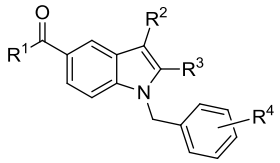

SR-9034 Analogs

SR#	CID	SID	R^1	R^2	R^3	R^4	IC_{50} (nM) Lanthascreen	EC_{50} (nM) PPRE Luc
9034	46233002	124349300		Me	Me	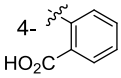	0.37	0.54 (15%)
1664	53239856	124349301	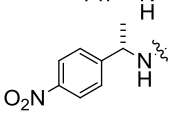	Me	Me	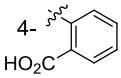	80	NA (0%)
1809	53239857	124349302	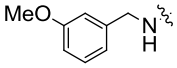	Me	Me	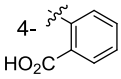	4	3 (15%)
1824	53239853	124349303	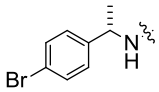	Me	Me	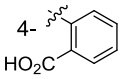	24	NA (0%)
2049	49852651	104223105		Me	Me	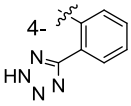	6	2 (23%)
2046	49852647	104223102		Me	Me	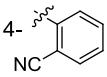	0.54	0.5 (24%)
2220	51049626	118043694		H	H	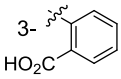	6	116 (17%)
2222	51049629	118043696		H	H	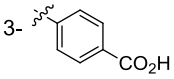	2	2 (16%)
1991	53239858	124349305		Me	Me	4-Cl	29	21 (15%)

Rosiglitazone IC_{50} = 18 nM; EC_{50} = 7.4 nM (100%)

3.5 Cellular Activity

Following the binding and transcriptional characterization of probe ML244, we next assessed its impact on phenotypes relevant to metabolism and diabetes. As shown in **Figure 10**, probe ML244 is active in a variety of cell-based assays performed by the assay provider.

***in vitro* functional analysis of ML244**

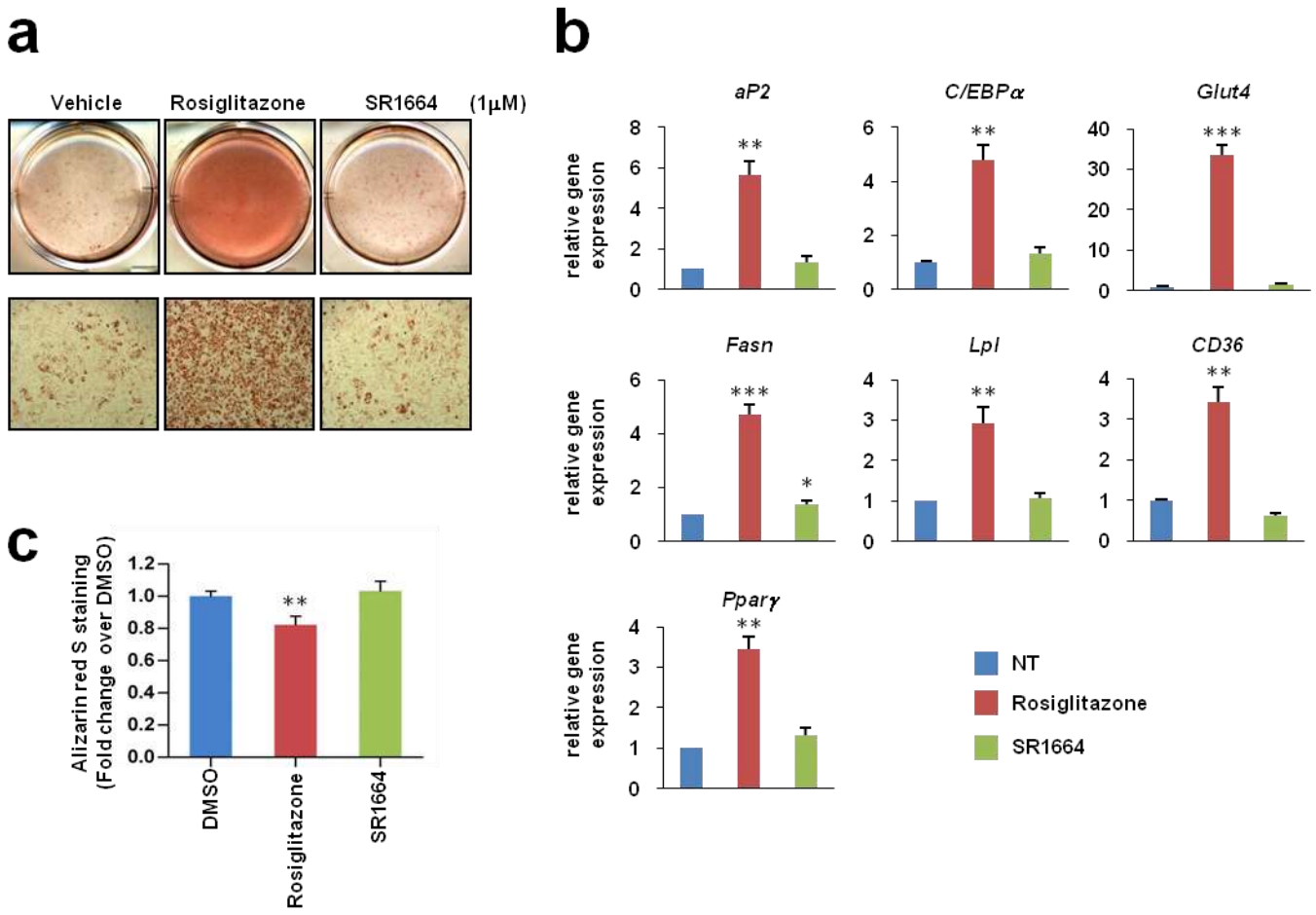

Figure 10. a, Lipid accumulation in differentiated 3T3-L1 cells treated with rosiglitazone or ML244 following Oil-Red-O staining. **b**, Expression of adipocyte-enriched genes in these cells was analyzed by qPCR (n=3). **c**, Mineralization of MC3T3-E1 osteoblast cells as determined by Alizarin Red S staining as measured 21 days post-differentiation (rosiglitazone: 10μM; ML244: 10μM). Error bars are S.E.M.; **p*<0.05, ***p*<0.01, ****p*<0.001, n.s.; not significant. NT, no treatment. These results are available in PubChem in AIDs 540286, 540287, 540289, 540290, 540291, 540292, and 540294.

Effects of PPARγ ligands on osteoblast gene expression

In contrast to full agonists, partial agonists are reported to show fewer side effects in preclinical models of diabetes, while retaining similar pharmacodynamic efficacy as TZDs. However, any level of classical activation of PPARγ is likely to drive plasma volume expansion (PVE) and modulation of bone formation. As a result, we wanted to assess whether probe ML244 altered the expression of genes involved in osteoblast differentiation. Quantitative RT-PCR (qPCR) analysis of alkaline phosphatase (*Alp*), Receptor activator of nuclear factor kappa-B ligand (*Rankl*), type I collagen (*Col1*) and PPAR-γ expression in MC3T3-E1 cells cultured in α-minimal essential medium (α-MEM) supplemented 200 µM ascorbic acid and 10 mM β-glycerophosphate for 7 days. The cells were treated with DMSO, rosiglitazone (10µM) or ML244 (10µM) at the start of differentiation. The gene expression was normalized to GAPDH. *p<0.05; **p<0.01; ***p<0.001. These results are shown in **Figure 11** and are available in PubChem in AIDs 540285 (ALP), 540283 (RANKL), 540284 (COLI), and PPARγ (540282). Importantly, and in agreement with probe ML244 acting as a PPARγ non-agonist ligand, we found that ML244 did not modulate expression of these genes, suggesting that it will not cause the side effects associated with current PPARγ full agonists.

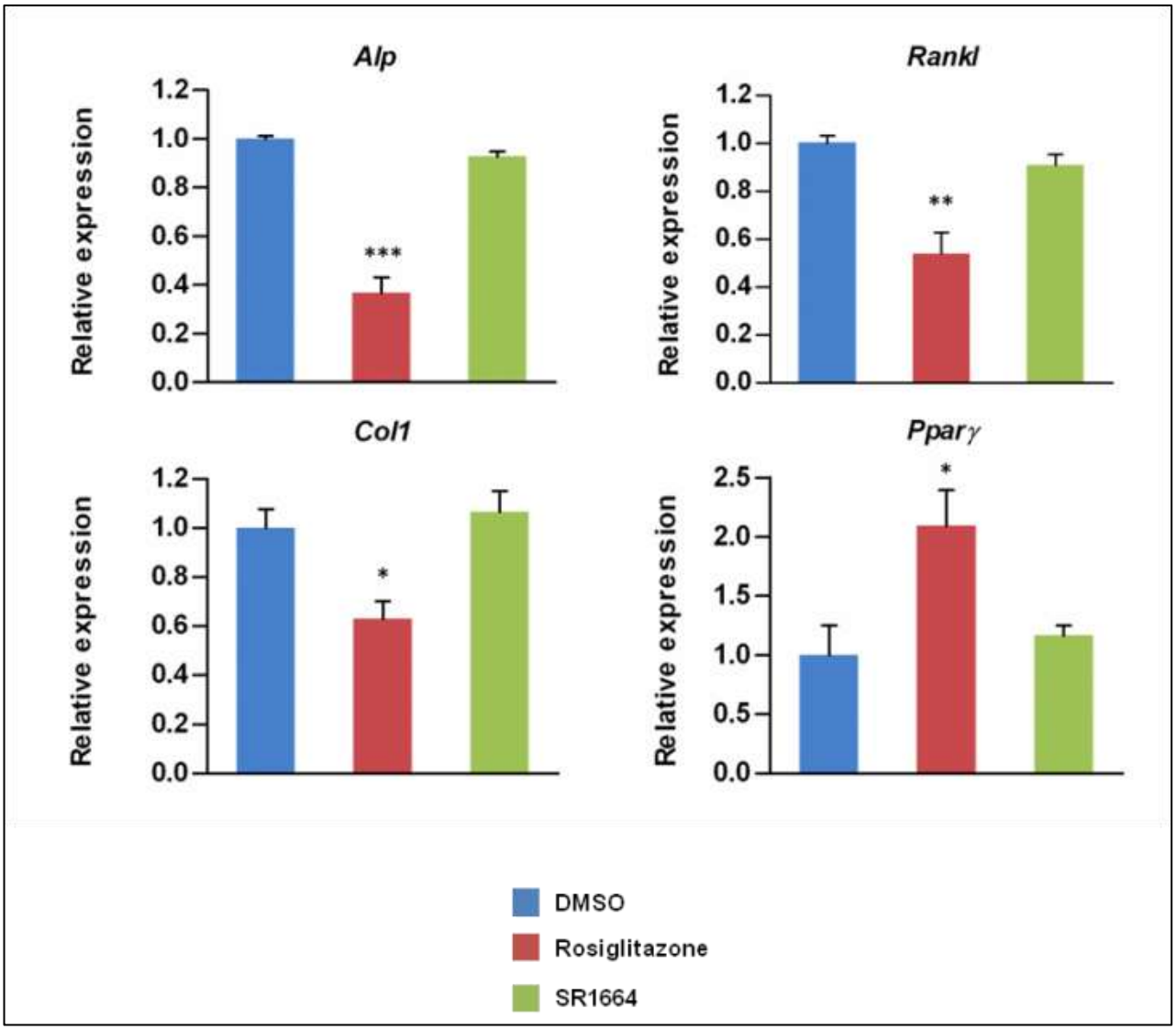

Figure 11. Effect of Probe ML244 on expression of genes involved with osteoblast differentiation.

3.6 Profiling Assays

We next assessed the selectivity of probe ML244 (1664) against other nuclear receptors [42]. While ML244 is inactive in transactivation of full length wild type PPARγ (AID 504939), it demonstrates very weak activation of the chimeric GAL4-PPARγ Ligand Binding Domain (LBD) receptor. Given the lack of translation of this weak activity to full length receptor, the minimal activation of PPARA and PPARD is of no concern (**Figure 12**).

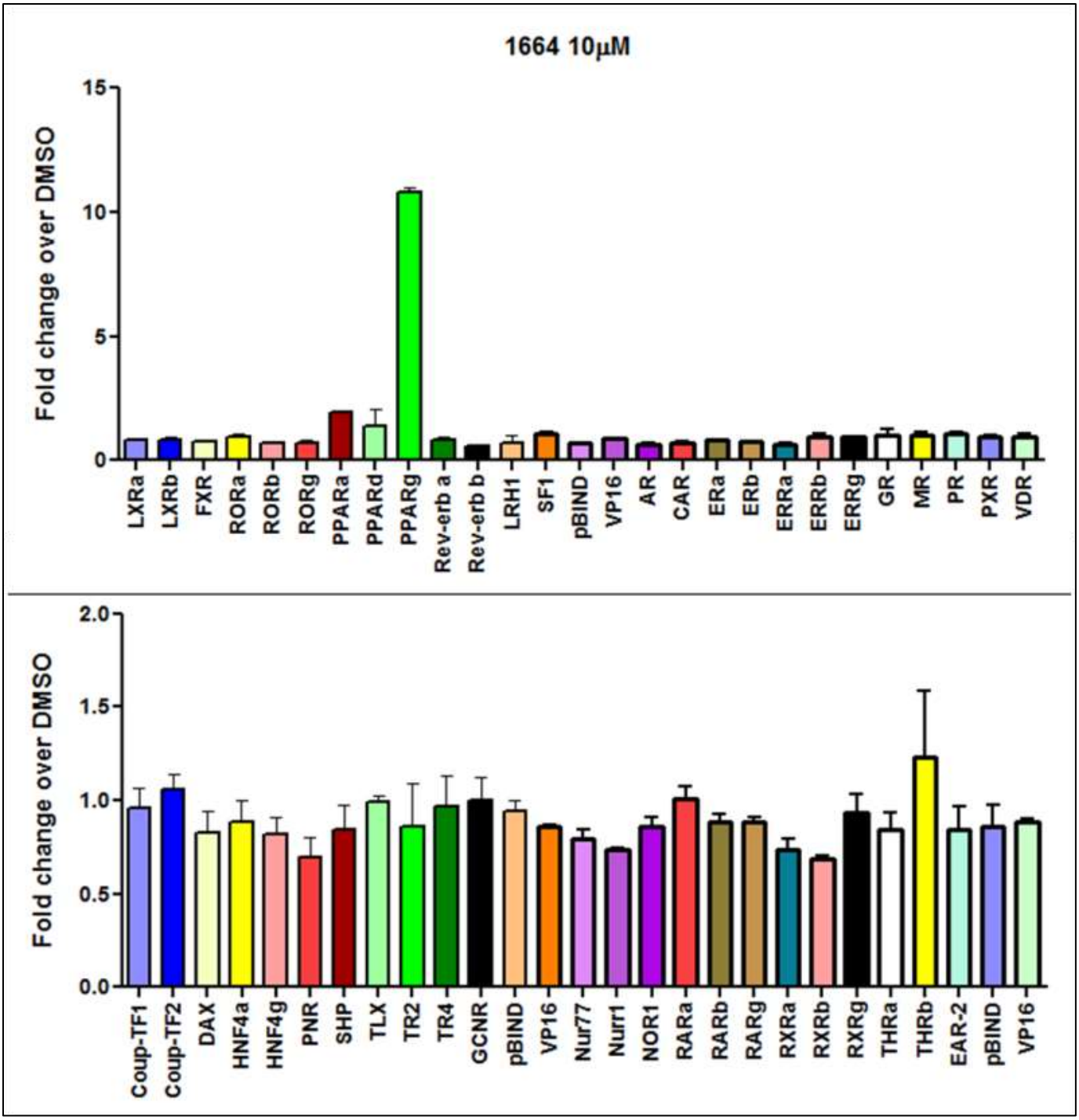

Figure 12. Selectivity screening of ML244 against a collection of > 50 mammalian nuclear receptors.

4 Discussion

4.1 Comparison to existing art and how the new probe is an improvement

The new probe ML244 is a significant improvement over prior art compound rosiglitazone in part because ML244 is a potent binder but non-agonist of PPARγ. ML244 potently blocks cdk5-dependent phosphorylation of PPARγ. There are no published potent binding, non-agonists that block cdk5-dependent phosphorylation of PPARγ. This is an important finding, given that many PPARγ-based drugs have a separate biochemical activity that includes the blocking of obesity-associated phosphorylation of PPARγ by Cdk5. As indicated in **Table 4**, probe ML244 offers a chemical scaffold distinct from that of rosiglitazone, and so may represent a starting point for further structural modifications and improvements in efficacy.

Table 4. Structural Comparison of Probe ML244.

Compound	Structure	CID	*PPAR*γ IC50	PubChem Activity Profile
Probe ML244 (SR-03000001664)	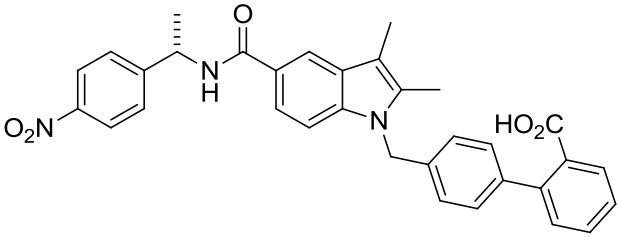	53239856	80 nM	Active in 15 of 230 assays (6.5%)
Prior art: Rosiglitazone	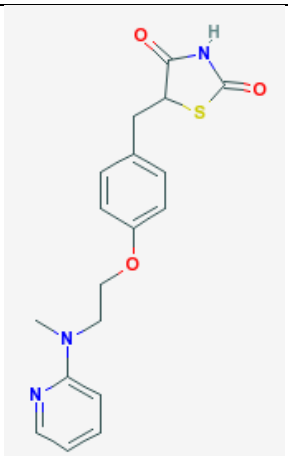	77999	0.009 µM	Active in 4 of 72 assays (5.5%)
MRL24	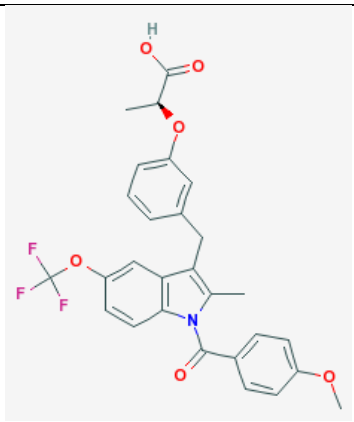	9958543 (SID 26750374)	2 nM (PMID 19507861)	Tested in 20 PubChem Bioassays (ChEMBL)

4.2 Mechanism of Action Studies

PPARγ activates transcription when ligand binding induces perturbation in receptor conformational ensemble, which leads to displacement of corepressor proteins (if bound) and the recruitment of coactivator proteins which either have intrinsic chromatin remodeling activity or they tether HATs.[9] PPARγ ligands bind in a relatively large cavity within the C-terminal ligand binding domain (LBD) of the receptor, which contains a ligand-regulated activation function (AF2) structural element that consists of helix 3–4 loop and helix 12 and is the site of co-activator binding. The activation mechanism involves global stabilization of the LBD and stabilization of the C-terminal helix 12 of AF2 upon ligand binding [19]. However, a number of **partial agonists** were shown to differentially stabilize various regions of the LBD [18]. They have a distinct physical interaction with the receptor resulting in diminished stabilization of the AF2 surface. X-ray structures of the PPARγ LBD liganded with full agonist rosiglitazone indicate hydrogen bonding between rosiglitazone and the side chain of Tyr 473 in helix 12 [20]. In contrast to rosiglitazone, the majority of selective PPARγ modulators (SPPARγMs) do not bind within hydrogen-bonding distance of Tyr 473, [21] suggesting that Tyr473 is a critical site of interaction for full agonists only. Currently, there are no crystal structures for our novel high affinity non-agonists of PPARγ.

Mode of action of non-agonists on PPARγ

Co-crystallography, mutagenesis and hydrogen/deuterium exchange (HDX) have all demonstrated that full agonists of PPARγ affect critical hydrogen bonds within the C-terminal helix (H12) of the receptor[18, 20, 22, 23]. This interaction stabilized the AF2 surface (helix 3-4 loop, C-terminal end of H11 and H12) of the receptor facilitating co-activator interactions. Interestingly, high affinity partial agonists have been identified that do not make these interactions yet still possess some level of classical agonism, and several of these have been shown to bind the backbone amide of S342 (S370 in PPARγ2) within the beta-sheet of the LBD[18]. More recently, Choi et al. demonstrated that the proximity of ligand to the amide of S342 correlated with increased stability of the helix 2-helix 2' loop, the region of the receptor containing S273 (S245 in PPARγ1) as determined by HDX[4]. We therefore sought to understand how PPARγ ligands devoid of classical agonism affect the conformational mobility of PPARγ. Surprisingly, HDX analysis of ML244 and SR1824 demonstrated that these compounds increased the conformational mobility of the C-terminal end of H11, a helix that abuts H12; in contrast, the full and partial agonists stabilized the same region of H11 (see **Figures 13** and **14**).

		Gamma 1		Gamma 2		2□□Structure				
	z	Start	End	Start	End		Rosiglitazone	MRL24	SR1664	SR1824
LRALAKHLYDSY	3	211	222	239	250	H1	0 (1)	1 (1)	0 (1)	0 (1)
RALAKHLYDS	3	212	221	240	249	H1	0 (0)	0 (0)	0 (1)	0 (1)
RALAKHLYDSY	3	212	222	240	250	H1	1 (1)	1 (0)	0 (1)	0 (1)
IKSFPLTKAKARAIL	3	223	237	251	265	H1-H2	-10 (2)	-5 (2)	-8 (3)	-7 (2)
TGKTTDKSPFVIYDM	3	238	252	266	280	Loop (pS)	-5 (2)	-5 (2)	0 (3)	-1 (3)
TGKTTDKSPFVIYDMNSLM	3	238	256	266	284	Loop (pS)	-4 (2)	-6 (2)	1 (3)	-1 (3)
MGEDKIKFKHITPLQEQSKE	3	257	276	285	304	H2'	0 (2)	-1 (2)	1 (3)	-2 (2)
MGEDKIKFKHITPLQEQSKEVA	3	257	278	285	306	H2'	0 (3)	-1 (3)	1 (3)	0 (3)
KIKFKHITPLQEQSKEVA	3	261	278	289	306	H2'	1 (3)	-1 (3)	1 (4)	0 (3)
IRIFQGCQ	2	279	286	307	314	H3	-67 (5)	-80 (2)	-37 (4)	-58 (3)
FRSVE	2	287	291	315	319	H3	-53 (7)	-82 (3)	-32 (4)	-59 (3)
RSVEAVQEITEYAKSIPGFVNL	3	288	309	316	337	H3	-19 (1)	-20 (1)	-15 (1)	-17 (1)
AVQEITE	1	292	298	320	326	H3	-22 (1)	-27 (1)	-19 (2)	-20 (2)
VQEITE	1	293	298	321	326	H3	-18 (1)	-20 (2)	-16 (1)	-16 (2)
YAKSIPGF	2	299	306	327	334	H3-H4	0 (0)	1 (1)	0 (0)	-1 (1)
YAKSIPGFVNL	2	299	309	327	337	H3-H4	-1 (1)	1 (1)	0 (1)	0 (1)
DLNDQVTL	1	310	317	338	345	H5	0 (1)	0 (1)	0 (1)	-1 (1)
DLNDQVTLL	2	310	318	338	346	H5	0 (1)	0 (1)	0 (1)	0 (1)
LKYGVHE	2	318	324	346	352	H5	-9 (1)	-2 (1)	-1 (1)	-2 (1)
LKYGVHEIIY	2	318	327	346	355	H5	-3 (0)	0 (1)	-1 (1)	-1 (0)
LKYGVHEIIYTM	3	318	329	346	357	H5	-2 (1)	0 (1)	0 (1)	-1 (1)
LASLMNKDGVL	2	330	340	358	368	sheet	-5 (1)	-4 (1)	-3 (1)	-4 (1)
ASLMNKDGVL	2	331	340	359	368	sheet	-6 (1)	-6 (1)	-4 (1)	-4 (1)
MNKDGVL	2	334	340	362	368	sheet	-6 (1)	-7 (1)	-4 (1)	-4 (2)
ISEGQGFMTRE	2	341	351	369	379	sheet-H6	-16 (2)	-22 (2)	-16 (3)	-16 (3)
ISEGQGFMTREFL	2	341	353	369	381	sheet-H6	-13 (2)	-18 (2)	-12 (2)	-13 (2)
ISEGQGFMTREFLKSLRKPFGDF	3	341	363	369	391	sheet-H6	-12 (2)	-16 (3)	-9 (2)	-8 (3)
FLKSLRKPFGD	2	352	362	380	390	H6-link	-2 (1)	-1 (1)	-3 (2)	-3 (2)
FLKSLRKPFGDFMEPKFEF	3	352	370	380	398	H6-H7	-10 (2)	-16 (1)	-5 (2)	-6 (2)
LRKPFGDF	2	356	363	384	391	H6-H7	-5 (2)	-18 (2)	-2 (3)	-3 (2)
LRKPFGDFMEPKFEF	3	356	370	384	398	H6-H7	-12 (1)	-18 (1)	-5 (2)	-5 (2)
AVKFNAL	2	371	377	399	405	H7	-9 (1)	-2 (1)	-2 (1)	-1 (2)
AVKFNALELDDSDL	2	371	384	399	412	H7-H8	-4 (1)	-1 (2)	0 (1)	1 (1)
NALELDDSDL	1	375	384	403	412	H7-H8	-1 (1)	-1 (1)	1 (2)	2 (1)
LELDDSDL	1	377	384	405	412	link-H8	0 (1)	-1 (1)	1 (1)	0 (1)
VIILSGDRPGLL	2	390	401	418	429	H8	-5 (1)	-1 (1)	-1 (1)	-1 (2)
VIILSGDRPGLLNVKPIED	3	390	408	418	436	H8	-2 (1)	-1 (1)	-1 (2)	-2 (2)
VIILSGDRPGLLNVKPIEDIQDNL	3	390	413	418	441	H8	-1 (1)	1 (2)	0 (1)	-1 (1)
IILSGDRPGLL	2	391	401	419	429	H8	-5 (1)	-2 (1)	0 (1)	-2 (2)
IILSGDRPGLLNVKPIE	3	391	407	419	435	H8-H9	-3 (1)	-1 (1)	0 (1)	-2 (1)
IILSGDRPGLLNVKPIED	3	391	408	419	436	H8-H9	-2 (2)	-1 (1)	0 (1)	-1 (1)
IILSGDRPGLLNVKPIEDIQDNL	3	391	413	419	441	H8-H9	-1 (1)	0 (1)	0 (1)	-1 (1)
NVKPIED	2	402	408	430	436	H9	0 (1)	0 (1)	4 (4)	0 (1)
NVKPIEDIQDNL	2	402	413	430	441	H9	0 (0)	1 (0)	1 (2)	0 (1)
NVKPIEDIQDNLLQA	2	402	416	430	444	H9	0 (0)	1 (1)	0 (0)	0 (1)
IQDNLL	1	409	414	437	442	H9	0 (1)	0 (1)	1 (0)	1 (1)
LELQLKLNHPESSQL	3	417	431	445	459	H9-H10	0 (1)	0 (1)	0 (1)	0 (1)
ELQLKLNHPESSQL	2	418	431	446	459	H9-H10	1 (1)	0 (1)	2 (2)	1 (1)
QLKLNHPESSQL	2	420	431	448	459	H9-H10	1 (2)	0 (2)	0 (3)	1 (2)
LKLNHPESSQL	2	421	431	449	459	H9-H10	1 (2)	-1 (2)	2 (3)	0 (2)
KLNHPESSQL	2	422	431	450	459	H9-H10	1 (2)	-1 (2)	2 (3)	0 (3)
FAKLLQKMTDL	2	432	442	460	470	H10	-2 (1)	-1 (1)	-1 (3)	-1 (1)
FAKLLQKMTDLRQ	3	432	444	460	472	H10-H11	-4 (1)	0 (1)	N/A	-3 (1)
LQKMTDL	2	436	442	464	470	H10-H11	-3 (1)	-1 (1)	0 (2)	-2 (1)
LQKMTDLRQ	3	436	444	464	472	H10-H11	-6 (1)	0 (1)	N/A	-1 (2)
RQIVTE	2	443	448	471	476	H11	-32 (1)	0 (2)	6 (2)	7 (2)
RQIVTEHVQL	3	443	452	471	480	H11	-36 (1)	-11 (2)	4 (3)	5 (3)
LQVIKKTETDM	2	453	463	481	491	H11	-5 (4)	-8 (3)	2 (4)	-1 (4)
LQVIKKTETDMSLHPLL	3	453	469	481	497	H11-H12	-7 (3)	-6 (3)	1 (4)	-1 (4)
LQVIKKTETDMSLHPLLQE	3	453	471	481	499	H11-H12	-8 (2)	-6 (3)	0 (4)	-2 (3)
IKKTETDMSLHPLL	3	456	469	484	497	H11-H12	-5 (3)	-1 (2)	1 (3)	-1 (3)
SLHPLLQEIYKDLY	2	464	477	492	505	H12	-26 (3)	-4 (7)	3 (5)	-2 (3)
HPLLQEIYKDLY	2	466	477	494	505	H12	-26 (4)	-5 (5.5)	1 (5)	0 (5)
QEIYKDLY	1	470	477	498	505	H12	-27 (3)	-6 (3)	5 (5)	1 (3)

Figure 13. Differential Hydrogen-Deuterium Exchange (HDX) data for rosiglitazone, MRL24, probe ML244 and SR1848. The sequence of each PPAR peptide is given in the left column, along with charge state of the ion (z), and both the PPARγ1 (gamma 1) and PPARγ2 (gamma 2) start/end residue numbers. The %D values indicate the difference between the mean HDX value obtained from apo PPARγ LBD measured at 6 time points (10s, 30s, 60s, 300s, 900s, 3600s) minus the mean value obtained from the "ligand" data collected at the same time point. Each result shows the average of three replicate experiments.

The number in parentheses represents the standard deviation of the measurements. Residues S273 (PPARγ 2) and S342 (PPARγ1) are highlighted in red.

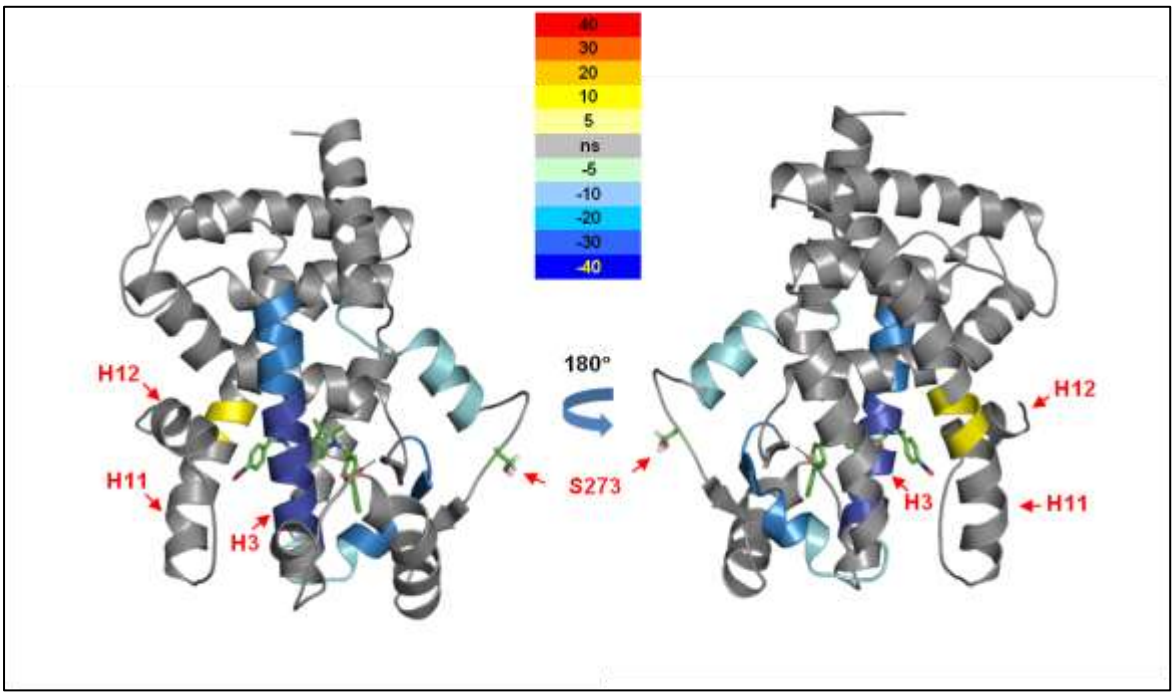

Figure 14. Overlay of differential HDX data onto the docking model of 2hfp bound to ML244. This overlay depicts the difference in HDX between ligand-free and ML244 bound PPARγ LBD. Perturbation data are color coded and plotted onto the backbone of the PDB file according to the key. Observed changes in HDX were statistically significant ($p<0.05$) in a two tailed t-test (n=3).

Next, we carried *out in silico* docking studies to understand the structural basis of ML244 interactions in the PPARγ1 ligand binding pocket and to correlate them with the perturbation observed by HDX (see **Figure 15**). In this model, the phenyl substituted nitro group of ML244 clashes with hydrophobic side chains of H11 such as Leu452 and Leu453 (Leu480 and Leu481 in PPARγ2, respectively) as well as Leu469 and Leu465 (corresponding to Leu497 and Leu493 in PPARγ 2) of the loop N-terminal to H12. This potentially explains the lack of stabilization of H12 and the destabilization of the region of H11 near His449 as seen by HDX. Despite the altered mode of binding, ML244 and rosiglitazone both bind to the same core residues within the PPARγ LBD as demonstrated by the ability of ML244 to attenuate the transcriptional activity of Rosiglitazone on PPARγ in the context of a competitive ligand binding assay.

Docking model of ML244 to PDB structure 2hfp.

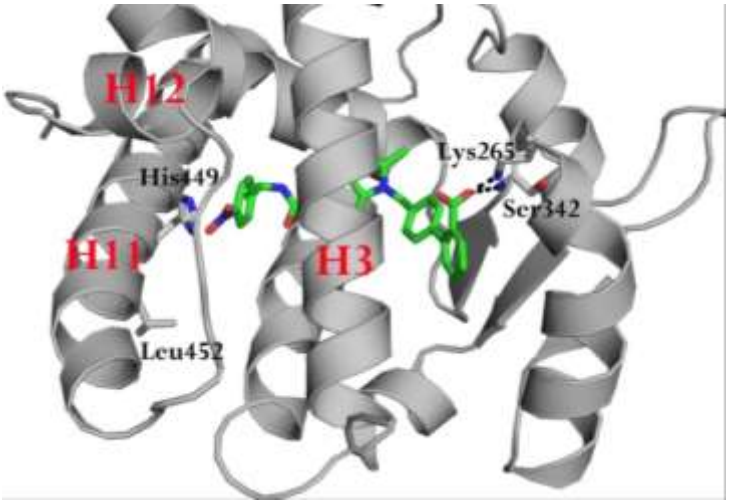

Figure 15. Docking model of ML244 to PDB structure 2hfp. Based on the docked structure, interactions of ML244 with the PPARγ ligand binding pocket can be classified into three basic epitope interaction locations: those of the ML244 carboxylic acid with the beta sheet region, the hydrophobic interactions of 1664 with H3, and the destabilizing interactions of ML244 with a small segment of H11 in close proximity to H12. Consistent with our HDX data shown below, ML244 makes polar contacts with the beta sheet as seen in many partial agonist structures. Specifically, the carboxylic acid of ML244 is within hydrogen bonding distance to the backbone nitrogen of Ser342 (3.36 Å) and the side chain nitrogen of Lys265 (2.70 Å) (corresponding to Ser370 and Lys293 in PPARγ2). Additionally, HDX has shown H3 to be highly stabilized by ML244. This can be explained by the hydrophobic nature of much of ML244 and its conformation in the binding pocket. ML244 is found wrapped around H3 in a horseshoe type conformation with many of its hydrophobic ring moieties making hydrophobic interactions with hydrophobic residues of H3. These residues include Cys285, Ile281, Phe282, Gly284, as well as the non-polar side chain region of Gln286. Perhaps most interesting is the binding mode of ML244 with the H11/H12 region. As with most partial agonists, ML244 makes no stabilizing hydrogen bond with Tyr473 (Tyr501 in PPARγ2) as seen with full agonists. The global location of ML244 places the phenyl substituted nitro group in proximity of H11 and H12 lending to areas of large clashing. Tyr473 of H12 and His449 of H11 both directly clash with this phenyl moiety. The docking model utilizes PPARγ1 numbering.

Next, we wanted to determine whether the altered transcriptional activity of probe ML244 may be attributed to differences in DNA binding or coactivator recruitment. To do this we compared the chromatin association of PPARγ or steroid receptor co-activator-1 (SRC-1) with the aP2 promoter using Chromatin Immunoprecipitation (ChIP). Rosiglitazone significantly increased PPARγ or SRC1 occupancy at the aP2 promoter. However, ML244 increased PPARγ recruitment to aP2 promoter, but not SRC1 (**Figure 16**). These results strongly suggest that ML244 has a different activity of co-regulator recruitment than rosiglitazone.

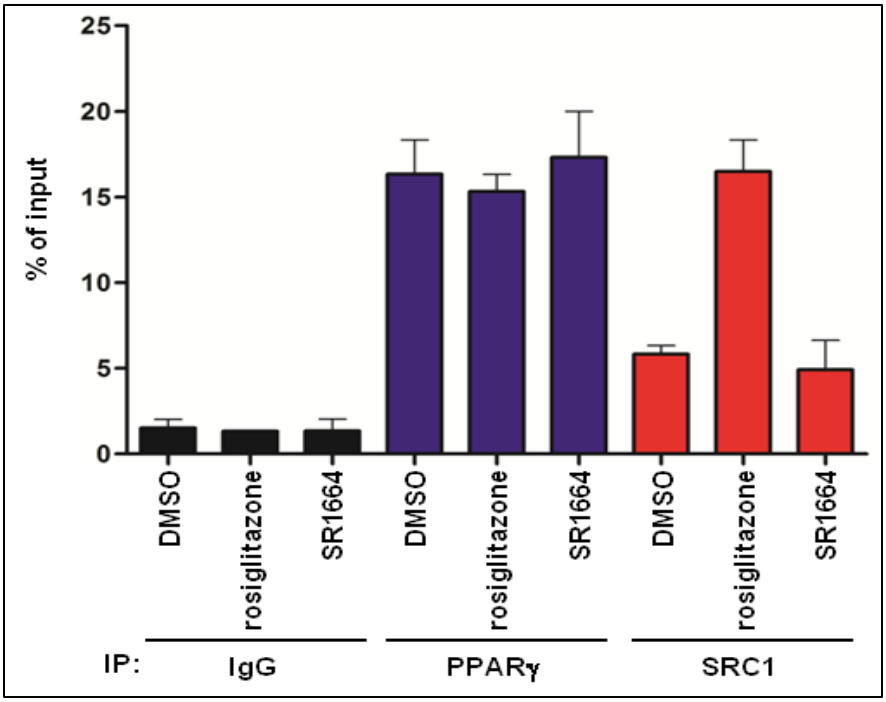

Figure 16. Quantitative PCR (qPCR) results were used to quantify enrichment of PPARγ or SRC1 at the aP2 promoter using chromatin immunoprecipitation (ChIP) assay.

We next compared the residue binding pattern of probe ML244 to that of Rosiglitazone to gain insights into the physical interactions taking place between these ligands and the receptor. As shown in **Figure 17**, we found that despite the altered mode of binding, probe ML244 and rosiglitazone both bind to the same core residues within the PPARγ LBD as demonstrated by the ability of ML244 to attenuate the transcriptional activity of Rosiglitazone on PPARγ in the context of a competitive ligand binding assay.

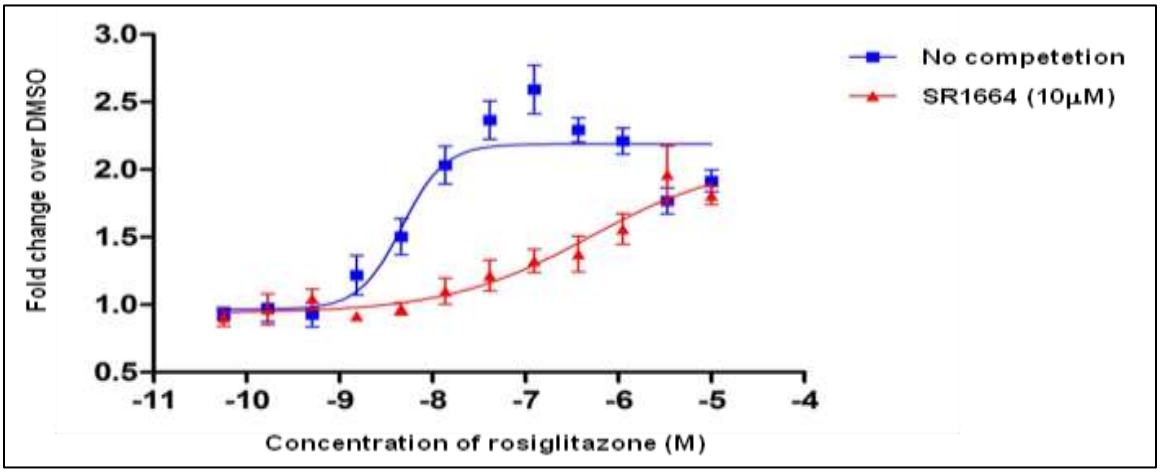

Figure 17. ML244 antagonizes the transcriptional agonism of rosiglitazone. These assays employed a ligand competition luciferase assay.

4.3 Planned Future Studies

The assay provider and SRIMSC are currently optimizing the physical properties and pharmacokinetic properties by making analogs of ML244. We are looking for analogs that are very potent binders (>50nM) with minimal transactivation activity (less than 4% at 1 µM compound relative to rosiglitazone). In addition, studies will also be employed to examine the *ex vivo* efficacy (3T3 L1 adipogenesis studies and MC3T3-E1 osteoblast studies) and *in vivo* action (ob/ob and DIO GTT studies) of analogs of the probe. In the *in vivo* studies we will profile gene expression patterns in fat depots to look for signatures that are regulated by cdk5 and signatures that are regulated by full agonists. These gene signatures will be surrogate markers for fully dissociated compounds. Finally, researchers in the broader scientific community will likely employ probe ML244 in assays to further elucidate the role of PPARγ in insulin sensitization.

5 References

1. Staels, B., J. Dallongeville, J. Auwerx, K. Schoonjans, E. Leitersdorf, and J.C. Fruchart, *Mechanism of action of fibrates on lipid and lipoprotein metabolism.* Circulation, 1998. **98**(19): p. 2088-93.PMID 9808609.
2. Berger, J.P., T.E. Akiyama, and P.T. Meinke, *PPARs: therapeutic targets for metabolic disease.* Trends Pharmacol Sci, 2005. **26**(5): p. 244-51.PMID 15860371.
3. Berger, J.P., A.E. Petro, K.L. Macnaul, L.J. Kelly, B.B. Zhang, K. Richards, A. Elbrecht, B.A. Johnson, G. Zhou, T.W. Doebber, C. Biswas, M. Parikh, N. Sharma, M.R. Tanen, G.M. Thompson, J. Ventre, A.D. Adams, R. Mosley, R.S. Surwit, and D.E. Moller, *Distinct properties and advantages of a novel peroxisome proliferator-activated protein [gamma] selective modulator.* Mol Endocrinol, 2003. **17**(4): p. 662-76.PMID 12554792.
4. Choi, J.H., A.S. Banks, J.L. Estall, S. Kajimura, P. Bostrom, D. Laznik, J.L. Ruas, M.J. Chalmers, T.M. Kamenecka, M. Bluher, P.R. Griffin, and B.M. Spiegelman, *Anti-diabetic drugs inhibit obesity-linked phosphorylation of PPARγamma by Cdk5.* Nature, 2010. **466**(7305): p. 451-6.PMID 20651683.
5. Lamotte, Y., P. Martres, N. Faucher, A. Laroze, D. Grillot, N. Ancellin, Y. Saintillan, V. Beneton, and R.T. Gampe, Jr., *Synthesis and biological activities of novel indole derivatives as potent and selective PPARγamma modulators.* Bioorg Med Chem Lett, 2010. **20**(4): p. 1399-404.PMID 20079636.
6. Grana, X., A. De Luca, N. Sang, Y. Fu, P.P. Claudio, J. Rosenblatt, D.O. Morgan, and A. Giordano, *PITALRE, a nuclear CDC2-related protein kinase that phosphorylates the retinoblastoma protein in vitro.* Proc Natl Acad Sci U S A, 1994. **91**(9): p. 3834-8.PMID 8170997.
7. Tontonoz, P., E. Hu, and B.M. Spiegelman, *Stimulation of adipogenesis in fibroblasts by PPAR gamma 2, a lipid-activated transcription factor.* Cell, 1994. **79**(7): p. 1147-56.PMID 8001151.
8. Lehmann, J.M., L.B. Moore, T.A. Smith-Oliver, W.O. Wilkison, T.M. Willson, and S.A. Kliewer, *An antidiabetic thiazolidinedione is a high affinity ligand for peroxisome proliferator-activated receptor gamma (PPAR gamma).* J Biol Chem, 1995. **270**(22): p. 12953-6.PMID 7768881.
9. Kliewer, S.A., J.M. Lenhard, T.M. Willson, I. Patel, D.C. Morris, and J.M. Lehmann, *A prostaglandin J2 metabolite binds peroxisome proliferator-activated receptor [gamma] and promotes adipocyte differentiation.* Cell, 1995. **83**(5): p. 813-819.PMID
10. Chawla, A., E.J. Schwarz, D.D. Dimaculangan, and M.A. Lazar, *Peroxisome proliferator-activated receptor (PPAR) gamma: adipose-predominant expression and induction early in adipocyte differentiation.* Endocrinology, 1994. **135**(2): p. 798-800.PMID 8033830.
11. Grey, A., M. Bolland, G. Gamble, D. Wattie, A. Horne, J. Davidson, and I.R. Reid, *The peroxisome proliferator-activated receptor-gamma agonist rosiglitazone decreases bone formation and bone mineral density in healthy postmenopausal women: a randomized, controlled trial.* J Clin Endocrinol Metab, 2007. **92**(4): p. 1305-10.PMID 17264176.
12. Kahn, S.E., B. Zinman, J.M. Lachin, S.M. Haffner, W.H. Herman, R.R. Holman, B.G. Kravitz, D. Yu, M.A. Heise, R.P. Aftring, and G. Viberti, *Rosiglitazone-Associated Fractures in Type 2 Diabetes.* Diabetes Care, 2008. **31**(5): p. 845-851.PMID

13. Lecka-Czernik, B., I. Gubrij, E.J. Moerman, O. Kajkenova, D.A. Lipschitz, S.C. Manolagas, and R.L. Jilka, *Inhibition of Osf2/Cbfa1 expression and terminal osteoblast differentiation by PPARγamma2.* J Cell Biochem, 1999. **74**(3): p. 357-71.PMID 10412038.
14. Nesto, R.W., D. Bell, R.O. Bonow, V. Fonseca, S.M. Grundy, E.S. Horton, M. Le Winter, D. Porte, C.F. Semenkovich, S. Smith, L.H. Young, and R. Kahn, *Thiazolidinedione use, fluid retention, and congestive heart failure: a consensus statement from the American Heart Association and American Diabetes Association.* Diabetes Care, 2004. **27**(1): p. 256-63.PMID 14693998.
15. Kahn, B.B. and T.E. McGraw, *Rosiglitazone, PPARγamma, and type 2 diabetes.* N Engl J Med, 2010. **363**(27): p. 2667-9.PMID 21190462.
16. Li, X., Y. He, C.H. Ruiz, M. Koenig, M.D. Cameron, and T. Vojkovsky, *Characterization of dasatinib and its structural analogs as CYP3A4 mechanism-based inactivators and the proposed bioactivation pathways.* Drug Metab Dispos, 2009. **37**(6): p. 1242-50.PMID 19282395.
17. Li, X., T.M. Kamenecka, and M.D. Cameron, *Bioactivation of the epidermal growth factor receptor inhibitor gefitinib: implications for pulmonary and hepatic toxicities.* Chem Res Toxicol, 2009. **22**(10): p. 1736-42.PMID 19803472.
18. Bruning, J.B., M.J. Chalmers, S. Prasad, S.A. Busby, T.M. Kamenecka, Y. He, K.W. Nettles, and P.R. Griffin, *Partial agonists activate PPARγamma using a helix 12 independent mechanism.* Structure, 2007. **15**(10): p. 1258-71.PMID 17937915.
19. Johnson, B.A., E.M. Wilson, Y. Li, D.E. Moller, R.G. Smith, and G. Zhou, *Ligand-induced stabilization of PPARγamma monitored by NMR spectroscopy: implications for nuclear receptor activation.* J Mol Biol, 2000. **298**(2): p. 187-94.PMID 10764590.
20. Nolte, R.T., G.B. Wisely, S. Westin, J.E. Cobb, M.H. Lambert, R. Kurokawa, M.G. Rosenfeld, T.M. Willson, C.K. Glass, and M.V. Milburn, *Ligand binding and co-activator assembly of the peroxisome proliferator-activated receptor-gamma.* Nature, 1998. **395**(6698): p. 137-43.PMID 9744270.
21. Oberfield, J.L., J.L. Collins, C.P. Holmes, D.M. Goreham, J.P. Cooper, J.E. Cobb, J.M. Lenhard, E.A. Hull-Ryde, C.P. Mohr, S.G. Blanchard, D.J. Parks, L.B. Moore, J.M. Lehmann, K. Plunket, A.B. Miller, M.V. Milburn, S.A. Kliewer, and T.M. Willson, *A peroxisome proliferator-activated receptor gamma ligand inhibits adipocyte differentiation.* Proc Natl Acad Sci U S A, 1999. **96**(11): p. 6102-6.PMID 10339548.
22. Hamuro, Y., S.J. Coales, J.A. Morrow, K.S. Molnar, S.J. Tuske, M.R. Southern, and P.R. Griffin, *Hydrogen/deuterium-exchange (H/D-Ex) of PPARγamma LBD in the presence of various modulators.* Protein Sci, 2006. **15**(8): p. 1883-92.PMID 16823031.
23. Chalmers, M.J., S.A. Busby, B.D. Pascal, M.R. Southern, and P.R. Griffin, *A two-stage differential hydrogen deuterium exchange method for the rapid characterization of protein/ligand interactions.* J Biomol Tech, 2007. **18**(4): p. 194-204.PMID 17916792.